

Probing New Physics from Top-charm Associated Productions at Linear Colliders

Junjie Cao^{a,b}, Guoli Liu^b, Jinmin Yang^{b,c}^a Department of Physics, Henan Normal University, Henan 453002, China^b Institute of Theoretical Physics, Academia Sinica, Beijing 100080, China^c Department of Physics, Tohoku University, Sendai 980-8578, Japan

(May 22, 2019)

The top-charm associated productions via e^+e^- , e^-e^- and e^-e^+ collisions at linear colliders, which are extremely suppressed in the Standard Model (SM), could be significantly enhanced in some extensions of the SM. In this article we calculate the full contribution of the topcolor-assisted technicolor (TC2) to these productions and then compare the results with the existing predictions of the SM, the general two-Higgs-doublet model and the Minimal Supersymmetric Model. We find that the TC2 model predicts much larger production rates than other models and the largest-rate channel is $!tc$, which exceeds 10 fb for a large part of the parameter space. From the analysis of the observability of such productions at the next-generation linear colliders, we find that the predictions of the TC2 model can reach the observable level for a large part of the parameter space while the predictions of other models are hardly accessible.

14.65Ha 12.60Jv 11.30Pb

I. INTRODUCTION

Since the measurements of top quark properties in Run I at the Fermilab Tevatron have small statistics, there remains plenty of room for new physics in the top quark sector. This stimulates a lot of efforts in the study of the top quark as a probe of new physics. Theoretical studies show that the top quark processes are sensitive to new physics [1]. In some new physics models like the popular Minimal Supersymmetric Model (MSSM) and the topcolor-assisted technicolor (TC2) model [2], the top quark may have some exotic production and decay channels [3-15]. Among these exotic processes, one kind is induced by the flavor-changing neutral-current (FCNC) interactions, which are extremely suppressed in the SM but could be significantly enhanced in some extensions [5-15]. Searching for these exotic processes will serve as a good probe for new physics. Now such possibilities exist on our horizon: the ongoing Fermilab Tevatron collider, the upcoming CERN Large Hadron Collider (LHC) and the planned Next-generation Linear Collider (NLC) will allow to scrutinize the top quark nature [16].

Due to its rather clean environment, the NLC will be an ideal machine to probe new physics. In such a collider, in addition to e^+e^- collision, we can also realize e^-e^- collision and e^-e^+ collision with the photon beams generated by the backward Compton scattering of incident electron and laser beams [17]. The FCNC top-charm associated productions via e^+e^- , e^-e^- and e^-e^+ collisions will be a sensitive probe for different new physics models and should be seriously examined. While these processes have been studied thoroughly in the MSSM [10], the corresponding studies in the TC2 model are not complete: so far only the production at e^+e^- collision has been studied [13,14]. From the studies of these processes in the MSSM [10] we know that the e^+e^- collision channel has a much smaller rate than e^-e^- collision or e^-e^+ collision. So it is necessary to consider all the production channels to complete the calculations in TC2 models. This is one aim of this article.

The other aim of this article is to compare the tc production rates predicted by different new physics models. Such analysis will help to distinguish different models once the production rate is measured at the NLC.

The reason for examining the TC2 effects in such top quark processes is two-fold. One is that the TC2 model is a popular realization of the fancy idea of technicolor and remains a typical candidate for new physics in the direction of dynamical symmetry breaking. This model has not been excluded by experiments so far and will face the test at future collider experiments. The other reason is that the TC2 model may have richer top-quark phenomenology than other new physics models since it treats the top quark differently from other fermions. In fact, the TC2 model predicts some anomalous couplings for the top quark, among which the most notable ones occur in the flavor-changing sector [5]. So the TC2 model may predict a large top-charm associated production rate and hence distinguish it from other new physics models.

This paper is organized as follows. Sec. II presents the calculations of the top-charm associated productions in TC2 model at the NLC. Sec. III compares the TC2 results with the predictions of the two-Higgs-doublet model and the MSSM. A discussion on observability at the NLC is given in Sec. IV and the conclusion is given in Sec. V.

A. The relevant Lagrangian

Among various kinds of dynamically electroweak symmetry breaking models, the TC2 model [2] is specially attractive since it connects the top quark with the electroweak symmetry breaking (EWSB). In this model, the topcolor interactions make small contributions to the EWSB, but give rise to the main part of the top quark mass $(1 - \epsilon)m_t$ with a model-dependent parameter $0 < \epsilon < 1$. The technicolor interactions play a main role in the EWSB and the extended technicolor interactions give rise to the masses of the ordinary fermions including a very small portion of the top quark mass ϵm_t . This model predicts some scalars such as top-pions $(\phi_t^0; \phi_t^\pm)$, which are condensates of the third generation quarks and have strong couplings with the third generation quarks. The existence of these new particles can be regarded as a typical feature of the TC2 model. Another feature of the TC2 model is the existence of large flavor-changing couplings [5]. In TC2 models the topcolor interactions are non-universal and therefore do not possess a Glashow-Iliopoulos-Maiani (GIM) mechanism. This non-universal gauge interactions result in some FCNC vertices when one writes the interactions in the quark mass eigenbasis. Furthermore, the neutral scalars of TC2 model as tt condensates also exhibits the same FCNC vertices. For instance, the interactions of top-pions take the form

$$\frac{m_t}{2F_t} \frac{P}{w} \frac{F_t^2}{w} [iK_{UR}^{tt} K_{UL}^{tt} \bar{t}_L t_R^0 + P^- 2K_{UR}^{tt} K_{DL}^{bb} \bar{t}_R b_L^+ + iK_{UR}^{tc} K_{UL}^{tt} \bar{t}_L c_R^0 + P^- 2K_{UR}^{tc} K_{DL}^{bb} \bar{c}_R b_L^+ + \text{h.c.}]; \quad (1)$$

where F_t is the top-pion decay constant and $w = \frac{P}{2} = 174 \text{ GeV}$. It has been shown that the values of the coupling parameters can be taken as [5]

$$K_{UL}^{tt} = K_{DL}^{bb} = 1; \quad K_{UR}^{tt} = 1; \quad K_{UR}^{tc} = \frac{P}{2} \frac{1}{w^2}; \quad (2)$$

with a model-dependent parameter $\epsilon < 1$. In the following calculation, we will take $K_{UR}^{tc} = \frac{P}{2} \frac{1}{w^2}$ and take ϵ as a free parameter in the range $0 < \epsilon < 1$. The TC2 model also predicts a CP-even scalar h_t^0 , called top-Higgs [5], which is a tt bound state and analogous to the η' particle in low energy QCD. Its couplings to quarks are similar to that of the neutral top-pion except that the top-Higgs is CP-even while the neutral top-pion is CP-odd.

B. Analytical calculations

Since the TC2 contribution to the process $e^+e^- \rightarrow \gamma^*/Z^* \rightarrow tc$ in e^+e^- collision has already been calculated in the literature [13,14] and since compared with $\gamma^*/Z^* \rightarrow tc$, its rate is suppressed by the propagators of the intermediate photon and Z boson, we focus on the processes $\phi_t^0 \rightarrow tc$ in e^+e^- collision and $\phi_t^\pm \rightarrow tc$ in e^-e^+ collision. For completeness we will also take into account the process $e^+e^- \rightarrow e^+e^- \phi_t^0 \rightarrow e^+e^- tc$ for e^+e^- collision, where the ϕ_t^0 particles are radiated out from the e^- and e^+ beams. Although it is a high-order process compared with $e^+e^- \rightarrow \gamma^*/Z^* \rightarrow tc$, its contributions may not be underestimated since there is no s-channel suppression.

In TC2 model, the process $\phi_t^0 \rightarrow tc$ proceeds at loop-level by exchanging the top-pions or top-Higgs. The corresponding Feynman diagrams are shown in Fig. 1. Compared with the corresponding diagrams in the MSSM, the contributions of TC2 model involve additional s-channel contributions, as shown in Fig. 1(r). For the top-pion (top-Higgs) within the range between m_t and $2m_t$, the top-pion (top-Higgs) decays dominantly into tc [5]¹ and thus such s-channel contributions become dominant if the c.m. energy of e^+e^- collision is high enough to produce a real top-pion (top-Higgs). In this case the cross section of top-charm associated production in the TC2 model may be quite large. In our calculation, we have considered all the decay channels of the top-pion and top-Higgs and taken into account the width effects in the s-channel propagators.

The magnitude of $\phi_t^0 \rightarrow tc$ can be written as

$$M = \frac{e^2 m_t^2}{16 F_t^2} \frac{V^2}{V^2} \frac{F_t^2}{V^2} K_{UR}^{tt} K_{UR}^{tc} \sum_i X_{it} u_{ti} \frac{1 + \epsilon}{2} v_c \prod_{j=1}^n (k_{1j} + i\Gamma_j) \prod_{j=2}^n (k_{2j} + i\Gamma_j); \quad (3)$$

¹ Depending on their masses, the decay products of neutral top-pion and top-Higgs may be tt , tc , bb , gg , W^+W^- , Z^0Z^0 , and Z^0 . Generally speaking, the dominant decay mode is tt for $m_{\phi_t^0} > 2m_t$, tc for $m_t < m_{\phi_t^0} < 2m_t$ and bb for $m_{\phi_t^0} < m_t$, respectively.

where the sum is over all Feynman diagrams and for each diagram F_i takes the form

$$\begin{aligned}
\mathcal{M}_i = & C_{i;1} P_t P_t + C_{i;2} P_c P_c + C_{i;3} P_t P_c + C_{i;4} P_t P_c + C_{i;5} P_t + C_{i;6} P_c + C_{i;7} P_c + C_{i;8} P_t + C_{i;9} G \\
& + C_{i;10} + C_{i;11} P_t P_t \mathbb{K}_2 + C_{i;12} P_c P_c \mathbb{K}_2 + C_{i;13} P_t P_c \mathbb{K}_2 + C_{i;14} P_t P_c \mathbb{K}_2 + C_{i;15} P_t \mathbb{K}_2 \\
& + C_{i;16} P_c \mathbb{K}_2 + C_{i;17} P_c \mathbb{K}_2 + C_{i;18} P_t \mathbb{K}_2 + C_{i;19} G \mathbb{K}_2 + C_{i;20} i'' k_2 : \quad (4)
\end{aligned}$$

Here, $k_{1,2}$ denote the momentum of incoming photons and $p_{t,c}$ the momentum of outgoing top and charm quarks. The $C_{i;j}$ ($j = 1, \dots, 20$) can be obtained by a straightforward calculation of each Feynman diagram. Their explicit expressions are presented in the Appendix.

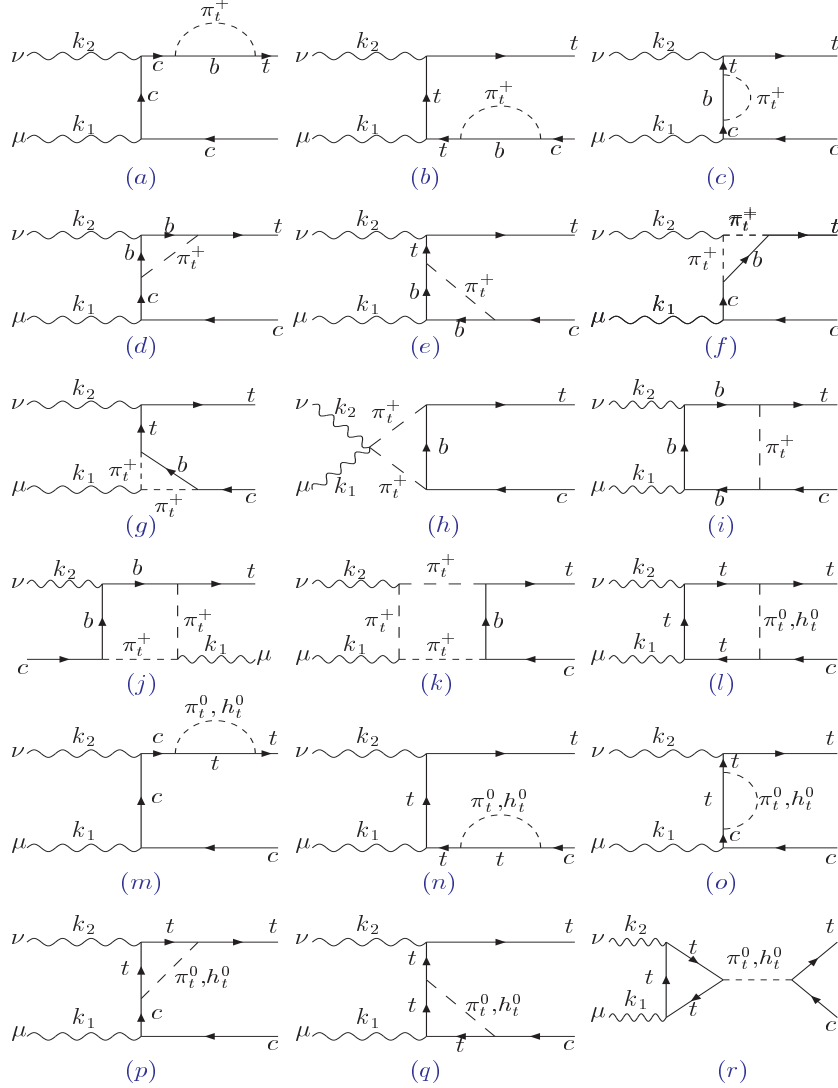


FIG. 1. Feynman diagrams contributing to the process $e^+e^- \rightarrow tc$ in the TC2 model. Those obtained by exchanging the two external photon lines are not displayed here.

We checked that all ultraviolet divergences cancel out in our results, which is essentially guaranteed by the renormalizability. We also checked that our results satisfy the Ward identity, $k_1 \cdot \mathcal{M} = 0$ and $k_2 \cdot \mathcal{M} = 0$ with \mathcal{M} being the sum of \mathcal{M}_i . In fact, the s-channel contribution mediated by either top-pion or top-Higgs (shown in Fig.1 (r)) also satisfies the Ward identity separately. This fact enables one to consider the s-channel contribution separately, as in Ref [15]. For the convenience of our discussion, we will divide TC2 contributions into the s-channel contribution and the non s-channel contribution, the latter of which includes the contributions from the t-channel, u-channel, quartic as well as box diagrams.

The tc production in e^+e^- collision proceeds through the process $e^+e^- \rightarrow e^+e^-tc$, where the e^- -beam is

generated by the backward Compton scattering of incident electron- and laser-beam and the γ is radiated from electron beam. The subprocess $e^+e^- \rightarrow \gamma^* \rightarrow e^+e^-$ has the same Feynman diagrams as those shown in Fig. 1. In our calculation we use the Weizsacker-Williams approximation [18] which treats γ from electron beam as a real photon. Thus the cross section is given by

$$\hat{\sigma}_{e^+e^- \rightarrow \gamma^* \rightarrow e^+e^-}(s_{ee}) = \int_0^1 dx P_{\gamma/e}(x; E_e) \hat{\sigma}_{\gamma^* \rightarrow e^+e^-}(s = xs_{ee}); \quad (5)$$

where $P_{\gamma/e}(x; E_e)$ is the probability of finding a photon with a fraction x of energy E_e in an ultra-relativistic electron and is given by [18]

$$P_{\gamma/e}(x; E_e) = -\frac{1 + (1-x)^2}{x} \ln \frac{E_e}{m_e} \left[\frac{1}{2} + \frac{x}{2} \ln \left(\frac{2}{x} \right) + 1 + \frac{(2-x)^2}{2x} \ln \frac{2-x}{2x} \right]; \quad (6)$$

Note that the incoming electron may also radiate Z -boson to contribute to the process $e^+e^- \rightarrow \gamma^* \rightarrow e^+e^-$. However, such contribution is suppressed by the probability function of finding a Z -boson in an ultra-relativistic electron [19] and can be safely neglected.

As for $e^+e^- \rightarrow e^+e^- \gamma^* \rightarrow e^+e^- \gamma^* \rightarrow e^+e^-$ collision, its cross section can be obtained by folding $P_{\gamma/e}$ with $\hat{\sigma}_{\gamma^* \rightarrow e^+e^-}$ as done in Eq.(5),

$$\begin{aligned} \hat{\sigma}_{e^+e^- \rightarrow e^+e^- \gamma^* \rightarrow e^+e^-}(s_{ee}) &= \int_0^1 dx \int_0^1 dy P_{\gamma/e}(x; E_{e^+}) P_{\gamma/e}(y; E_{e^-}) \hat{\sigma}_{\gamma^* \rightarrow e^+e^-}(s = xys_{ee}) \\ &= \frac{1}{p_a} \int_0^1 2zdz \hat{\sigma}_{\gamma^* \rightarrow e^+e^-}(s = z^2 s_{ee}) \int_0^1 \frac{dx}{x} P_{\gamma/e}(x; E_{e^+}) P_{\gamma/e}\left(\frac{z^2}{x}; E_{e^-}\right); \end{aligned} \quad (7)$$

where we define $a = (m_t + m_c)^2 = s_{ee}$. In TC2 model, it is argued that the top-Higgs may couple directly with ZZ or W^+W^- [5]. If so, the processes $e^+e^- \rightarrow e^+e^- Z^* \rightarrow e^+e^- \gamma^* \rightarrow e^+e^-$ and $e^+e^- \rightarrow W^+W^- \rightarrow \gamma^* \rightarrow e^+e^-$ may also be important for top-charm associated production at e^+e^- collision [14]. We will take the results of Ref. [14] for comparison in our discussions.

For both e^+e^- collision and e^-e^+ collision, the photon beams are generated by the backward Compton scattering of incident electron- and laser-beams just before the interaction point. The events number is obtained by convoluting the cross section with the photon beam luminosity distribution. For e^+e^- collider the events number is obtained by

$$N_{\gamma^* \rightarrow e^+e^-} = \int_0^1 \frac{dL_{\gamma}}{d^3s} \frac{dL}{d^3s} \hat{\sigma}_{\gamma^* \rightarrow e^+e^-}(s) L_{ee} \hat{\sigma}_{ee}(s_{ee}); \quad (8)$$

where $dL_{\gamma} = d^3p_{\gamma}$ is the photon beam luminosity distribution and $\hat{\sigma}_{\gamma^* \rightarrow e^+e^-}(s_{ee})$, with s_{ee} being the energy-square of e^+e^- collision, is defined as the effective cross section of $\gamma^* \rightarrow e^+e^-$. In optimum case, it can be written as [21]

$$\hat{\sigma}_{\gamma^* \rightarrow e^+e^-}(s_{ee}) = \frac{1}{p_a} \int_0^{x_{max}} 2zdz \hat{\sigma}_{\gamma^* \rightarrow e^+e^-}(s = z^2 s_{ee}) \int_{z^2=x_{max}}^1 \frac{dx}{x} F_{\gamma/e}(x) F_{\gamma/e}\left(\frac{z^2}{x}\right); \quad (9)$$

where $F_{\gamma/e}$ denotes the energy spectrum of the back-scattered photon for unpolarized initial electrons and laser photon beams given by

$$F_{\gamma/e}(x) = \frac{1}{D(\gamma)} \left[1 - x + \frac{1}{1-x} - \frac{4x}{(1-x)^2} + \frac{4x^2}{(1-x)^3} \right]; \quad (10)$$

The definitions of parameters γ , $D(\gamma)$ and x_{max} can be found in [21]. In our numerical calculation, we choose $\gamma = 4.8$, $D(\gamma) = 1.83$ and $x_{max} = 0.83$.

For the e^-e^+ collider the effective cross section of $e^+e^- \rightarrow \gamma^* \rightarrow e^+e^-$ is defined as

$$\begin{aligned} \hat{\sigma}_{e^+e^- \rightarrow \gamma^* \rightarrow e^+e^-}(s_{ee}) &= \frac{1}{L_{ee}} \int_0^1 \frac{dL_{\gamma}}{d^3s} \frac{dL_{e^-}}{d^3s_e} \hat{\sigma}_{\gamma^* \rightarrow e^+e^-}(s_e) \\ &= \frac{1}{p_a} \int_0^{x_{max}} 2zdz \hat{\sigma}_{\gamma^* \rightarrow e^+e^-}(s = z^2 s_{ee}) \int_{z^2=x_{max}}^1 \frac{dx}{x} P_{\gamma/e}(x; E_e) F_{\gamma/e}\left(\frac{z^2}{x}\right); \end{aligned} \quad (11)$$

>From above analysis, especially from Eqs.(7,9,11), we know the cross sections for $e^+e^- \rightarrow e^+e^- \gamma^* \rightarrow e^+e^-$, $e^+e^- \rightarrow \gamma^* \rightarrow e^+e^-$ and $\gamma^* \rightarrow e^+e^-$ are connected by convoluting the same $\hat{\sigma}_{\gamma^* \rightarrow e^+e^-}$ with different photon distribution functions. Noting the fact $F_{\gamma/e} > P_{\gamma/e}$ for the integrated range of x , one can infer that the cross section at e^-e^+ collider is the largest, which will be shown in our results. In the following the major part of discussions will be focused on the production in e^-e^+ collision.

The cross sections of top-charm associated productions in TC2 model depend on ϵ , the masses of top-pions and the mass of top-Higgs. ϵ parameterizes the strength of the flavor changing interaction and we vary it in the range of 0.01–0.1, as suggested in [5]. Since the mass splitting between the neutral top-pion and the charged top-pion comes only from the electroweak interactions and thus should be small, we assume $m_{\tilde{t}^0} = m_{\tilde{t}^\pm} = m_{\tilde{t}}$. Ref. [2] has estimated the mass of top-pions and showed that $m_{\tilde{t}}$ is allowed to be a few hundred GeV, depending on the details of the considered models. The mass of the top-Higgs h_t can be estimated in the Nambu–Jona-Lasinio (NJL) model in the large N_c approximation and is found to be about $2m_{\tilde{t}}$ [5]. This estimation is rather crude and the mass below the $\tilde{t}\tilde{t}$ threshold is quite possible in a variety of scenarios [22]. In our analysis we use M_{TC} ($m_{\tilde{t}} = m_{h_t}$) to denote the common value of these masses when not considering their difference. As for other involved parameters, we take $m_t = 174.3$ GeV, $V = 174$ GeV, $F_t = 50$ GeV and neglect the bottom and charm quark masses in numerical evaluation. Throughout this paper, the charge conjugate production channel, i.e., the $t\bar{c}$ production, is also included in our numerical results.

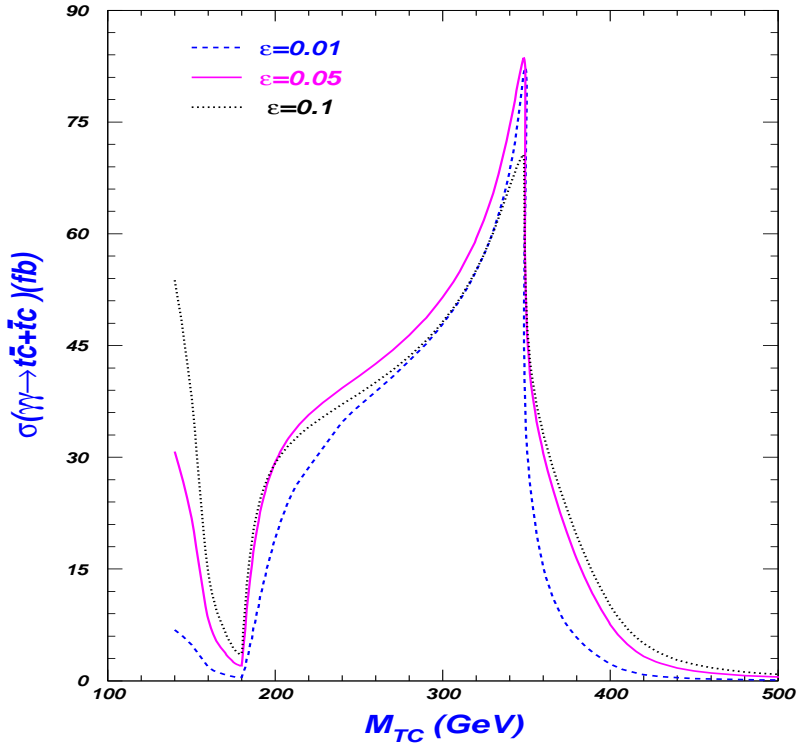


FIG. 2. The M_{TC} dependence of the cross section in e^+e^- collision with $\sqrt{s_{e^+e^-}} = 500$ GeV.

Fig 2 shows the dependence of the cross section of $\gamma \rightarrow t\bar{c} + t c$ on the TC2 scale with different values of ϵ . One sees that, as the scale gets high, the cross section first decreases for $M_{TC} < m_{\tilde{t}} + m_c$, then increases monotonously for $M_{TC} < 2m_{\tilde{t}}$ to arrive at its peaks at $M_{TC} = 2m_{\tilde{t}}$ with $\sigma_{max} = 70 \sim 80$ fb, and finally drops rapidly. This behavior may be explained as follows. For $M_{TC} < m_{\tilde{t}} + m_c$, the non s -channel contributions are dominant (in this region \tilde{t}^0 and h_t in the s -channel cannot be on-shell since they cannot decay to $t\bar{c}$) and such effects decrease with increasing M_{TC} as required by the decoupling theorem. So far this range of M_{TC} can not be ruled out by direct search of technicolor particles [23], but is disfavored by the constraints from R_b [24] which, however, is model dependent. For $m_{\tilde{t}} + m_c < M_{TC} < 2m_{\tilde{t}}$, $t\bar{c}$ becomes the dominant decay mode of \tilde{t}^0 and h_t , and the branching fraction increases as M_{TC} gets large. In this region the s -channel contributions are dominant and can be quite large since \tilde{t}^0 and h_t can be produced on-shell and then decay dominantly into $t\bar{c}$. For $M_{TC} > 2m_{\tilde{t}}$, although \tilde{t}^0 and h_t may still be produced on-shell (need high c.m. energy and thus suppressed by the photon luminosity distribution), the s -channel contributions get small since $\tilde{t}\tilde{t}$ becomes the dominant decay mode of \tilde{t}^0 and h_t . From the figure one can also see that, unlike other regions of M_{TC} where large ϵ leads to large cross section, in the region $m_{\tilde{t}} + m_c < M_{TC} < 2m_{\tilde{t}}$ the cross section is relatively insensitive to ϵ value and $\epsilon = 0.1$ does not correspond to the largest cross section. The reason is that ϵ affects both the total width and the partial width into $t\bar{c}$ of \tilde{t}^0 and h_t in the s -channel. There exists

competition between these two effects and as a result, the branching fraction into $t\bar{c}$ does not increase monotonously with μ .

Fig. 2 shows that the $t\bar{c}$ production rate in e^+e^- collision can exceed 10 fb in a large part of parameter space and maximally can reach 80 fb. Comparing with $e^+e^- \rightarrow t\bar{c}$ in e^+e^- collision, which can only reach 0.1 fb in TC2 model [13] due to the s -channel suppression, one may infer that the e^+e^- collision may be much better in probing TC2 model. We will elaborate the observability of the top-charm associated production at the NLC in Sec. IV. Since we only intend to figure out the typical order of the production rate for such rare processes, we $\mu = 0.1$ as an example in our following analysis.

Next we consider the case where the masses of the top-pions and the top-Higgs are not degenerate. Fig. 3 shows some plots of the cross section versus the mass of the top-pions for different top-Higgs mass values. For $m_{h_t} = 2000$ GeV, the contributions from the top-Higgs are small and the corresponding results in Fig. 3 can be regarded as the contributions from the top-pions. Taking this in mind, we infer from Fig. 3 that the contributions from the top-Higgs tend to enhance top-pion effects for the whole considered range of m_{π_t} except for a very light top-Higgs of 150 GeV. In case of such a light top-Higgs, there exists a small region in which the two kinds of contributions interfere destructively. Among the four values of m_{h_t} chosen in Fig. 3, $m_{h_t} = 300$ GeV gives the largest cross section, the reason of which has been explained in the paragraph following Fig. 2.

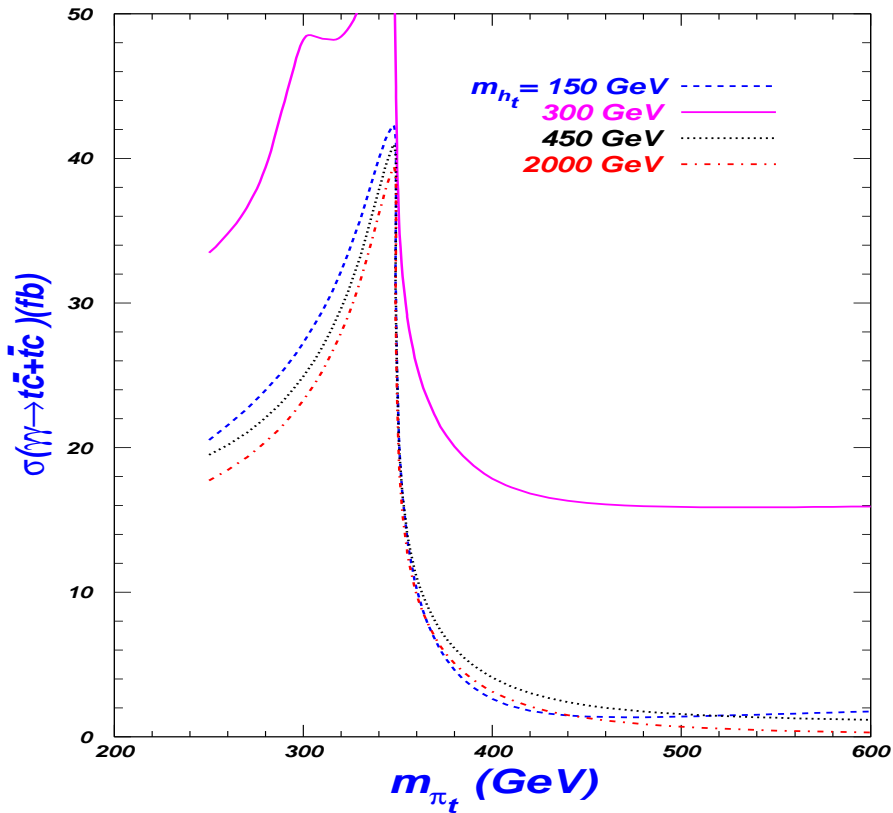


FIG. 3. The m_{π_t} dependence of the cross section of $e^+e^- \rightarrow t\bar{c} + t\bar{c}$ with different values of m_{h_t} for $\mu = 500$ GeV.

In Fig. 4, we plot the contours of the cross section in the plane of μ versus M_{TC} . One can learn that as long as the TC2 scale M_{TC} is lower than 500 GeV, there exists a large parameter space where the cross section can exceed 1 fb.

In Fig. 5, we show the behavior of the rates for $e^+e^- \rightarrow t\bar{c}$, $e^+e^- \rightarrow e^+e^- t\bar{c}$ and $e^+e^- \rightarrow e^+e^- t\bar{c}$ versus the collider energy. As illustrated in the figure, the $(e^+e^- \rightarrow t\bar{c})$ is insensitive to the collider energy for $E_{cm} > 400$ GeV while the other two channels rise significantly with the collider energy, which can be explained by the energy dependence of $P_{e^+e^-}$.

Fig. 5 shows that $(e^+e^- \rightarrow t\bar{c}) < (e^+e^- \rightarrow e^+e^- t\bar{c}) < (e^+e^- \rightarrow e^+e^- t\bar{c})$. Since the s -channel process $e^+e^- \rightarrow \gamma/Z \rightarrow t\bar{c}$ is suppressed by the propagators of the intermediate photon or Z -boson and was found [13] to occur at a similar rate as $e^+e^- \rightarrow e^+e^- t\bar{c}$, we conclude that the production rate in e^+e^- collision is largest at a linear collider.

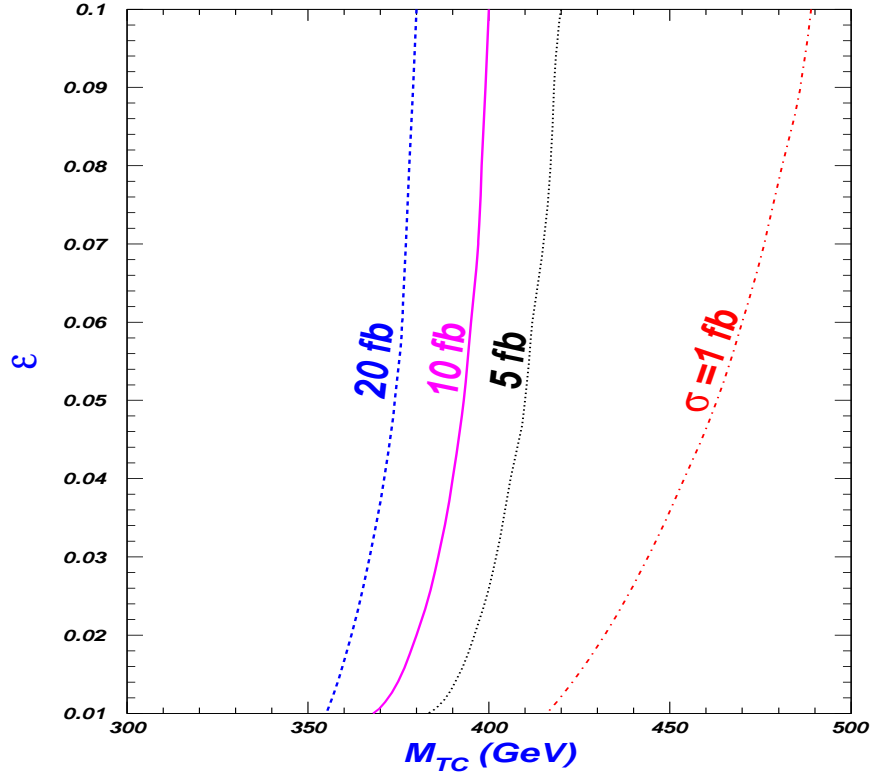


FIG .4. Contours of the cross section of $e^+e^- \rightarrow tc$ in the plane of ϵ versus M_{TC} for $\sqrt{s_{e^+e^-}} = 500 \text{ GeV}$.

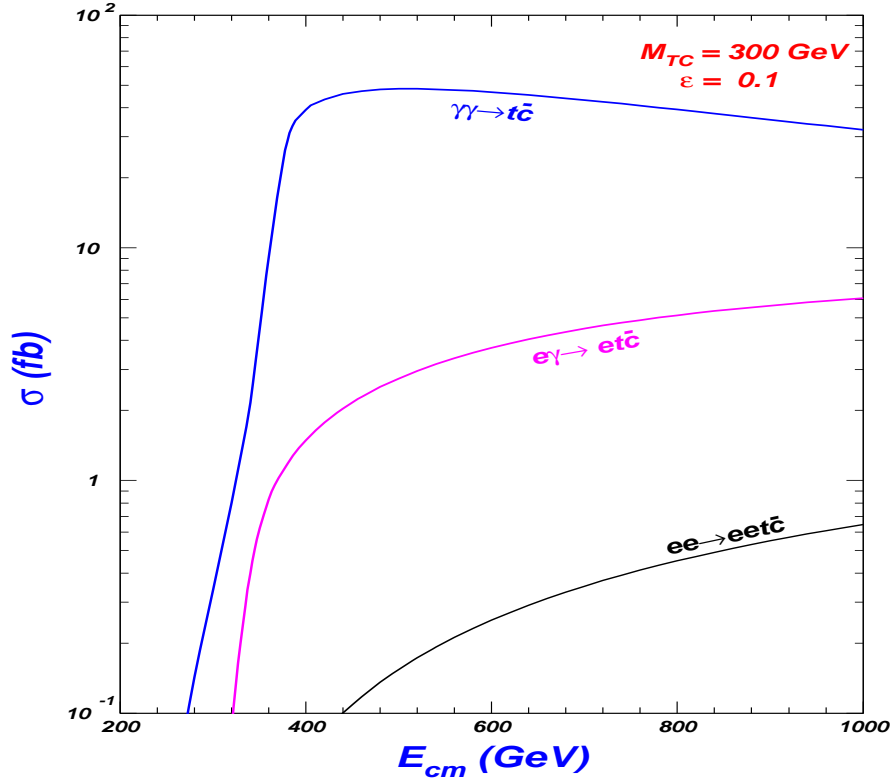


FIG .5. The cross sections of $\gamma \rightarrow tc$, $e\gamma \rightarrow etc$ and $e^+e^- \rightarrow e^+e^-tc$ versus the e^+e^- center-of-mass energy.

In this section, we first briefly recapitulate the sources of FCNC transitions in different models and then compare the typical magnitudes of various FCNC processes at the NLC predicted by different models. We arrive at the observation that the TC2 model predicts much larger FCNC transitions than other new physics models.

It is well known that in the SM the FCNC transitions are absent at tree-level and can occur only at loop level by the GIM mechanism. The source of such FCNC transitions is the non-diagonality of the Cabibbo-Kobayashi-Maskawa (CKM) matrix. In the extensions of the SM, although the CKM matrix can still induce additional contributions to FCNC via loops composed by new particles, some new sources for FCNC transitions usually come in.

As the simplest extension of the SM, the two-Higgs-doublet model (2HDM) may naturally have FCNC mediated by the Higgs bosons at tree-level, unless some ad hoc discrete symmetry is imposed. The generic type of 2HDM is the so-called "type-III" model (2HDM-III) [25,26], in which the up-type and down-type quarks couple to both Higgs doublets and thus the diagonalization of the quark mass matrices does not automatically ensure the diagonalization of the Yukawa couplings. In a popular realization of 2HDM-III, one Higgs doublet is responsible for the electroweak symmetry breaking as well as generating the fermion masses while the other doublet has FCNC couplings whose strength are usually parameterized as [25]

$$\kappa_{ij}^{U,D} = \kappa_{ij}^{U,D} \frac{p_{ij} m_i m_j}{v} \quad (12)$$

with $i, j = 1, 2, 3$ being the generation indices, m_i the quark masses and κ_{ij} the dimensionless parameters. From Eq.(12), we can learn the FCNC coupling without top quark is generally suppressed by the involved quark masses. One impressive feature of 2HDM-III is that the coupling strengths of the FCNC are related with those of flavor-changing charged currents. The FCNC couplings κ_{tc}^U and κ_{ct}^U then contribute to some low energy observable and the bounds from low energy data are $\kappa_{tc}^U, \kappa_{ct}^U = O(1)$ [26].

The MSSM [27] also contains two Higgs doublets. However, the homology of the superpotential requires that one doublet couple only to up-type quarks while the other doublet couple only to down-type quarks and hence avoids tree-level FCNC transitions in the Higgs sector. Note that when supersymmetry is broken, the couplings QUH_d and $QD H_u$ are generated at one-loop level to induce FCNC Yukawa couplings. While such FCNC couplings are generally small for up-type quarks, they may be quite large for down-type quarks due to the enhancement by large $\tan\beta$ [28]. Another source of FCNC in the MSSM is the flavor mixings of sfermions [27,29], which induce FCNC transitions in the fermion sector through loops composed by sparticles, such as sfermion-gaugino loop and sfermion-Higgsino loop [9].

As discussed in Sec. II, TC2 model, as one of the dynamical EW SB models, is quite different from the 2HDM and the MSSM. In this model, the scalar bosons are composite particles with properties quite similar to those of Higgs bosons. One distinguished character of TC2 model is that the third generation quarks are special and have new top-color interaction [2]. This non-universal top-color interaction can result in FCNC transitions when expressing the interactions in terms of quark mass eigenstates. In particular, the triangle texture of the up-type quark mass matrix due to the generic top-color breaking pattern can lead to large flavor mixing between t_R and c_R [5]. Furthermore, the FCNC transitions also exhibit themselves in the neutral scalar sector, which are tt condensates. Therefore, the top flavor phenomenology is much richer in this model than in other models.

So far as the top-charm associated productions are concerned, in the SM they are severely suppressed since they proceed through loops comprising of light down-type quarks (much lighter than top quark mass scale) and involving the small mixings between the third-generation quarks and the quarks of the first two generations. Table I shows the rates for $e^+e^- \rightarrow tc$, $e^+e^- \rightarrow tc$ etc and $e^+e^- \rightarrow tc$ at the NLC. As can be seen, the rates predicted by the SM are too small to be accessible at the NLC.

In 2HDM-III, the process $e^+e^- \rightarrow tc$ proceeds in a similar way to that in TC2 model except that the top-pions and top-Higgs in Fig. 1 should be replaced by the corresponding Higgs bosons. However, due to the smallness of κ_{tc}^U , its cross section is generally two orders lower than in the TC2 model. In Table I, we present the predictions of 2HDM-III for various production channels at the NLC. One impressive character is that the rates of $e^+e^- \rightarrow tc$ and $e^+e^- \rightarrow tc$ is comparable to $e^+e^- \rightarrow tc$ and much larger than $e^+e^- \rightarrow tc$. The reason is that in 2HDM-III the Higgs bosons may couple at tree-level with ZZ or W^+W^- and, consequently, despite of the suppression of the probability to find the gauge bosons in an electron, its cross section may still be large [32].

In the MSSM, $e^+e^- \rightarrow tc$ proceeds via the loops comprising of squarks, gluinos, charginos and neutralinos. The

corresponding results in Table I are taken from [10] where only SUSY-QCD contributions are considered². As shown in Table I, the cross sections in the MSSM, although can be much larger than the SM predictions, are generally much smaller than the TC2 predictions. The reason is twofold. One is that in the MSSM there is no s-channel contribution like that shown in Fig.1 (c) at one-loop level. The other reason is that there are cancellations between different diagrams due to the unitarity of the matrix diagonalizing the up-type squark mass matrix, which is often called the 'Super-GIM' mechanism.

Table I: Theoretical predictions for top-quark FCNC processes. The predictions of new physics models are optimum values. The e^+e^- collider energy is 500 GeV for production processes. The cross sections are in the units of fb. The processes not referenced are estimated by us.

	SM	2HDM -III	MSSM	TC2
$(t \rightarrow c)$	$O(10^{-8})$ [10]	$O(10^{-1})$ [12]	$O(10^{-1})$ [10]	$O(10)$
$(e \rightarrow \tau)$	$O(10^{-9})$ [10]	$O(10^{-2})$	$O(10^{-2})$ [10]	$O(1)$
$(e^+e^- \rightarrow t\bar{c})$	$O(10^{-10})$ [30,10]	$O(10^{-3})$ [31]	$O(10^{-2})$ [10]	$O(10^{-1})$ [13]
$(e^+e^- \rightarrow e^+e^- t\bar{c})$	$< 10^{-10}$ [10]	$O(10^{-3})$	$O(10^{-3})$ [10]	$O(10^{-1})$
$(e^+e^- \xrightarrow{Z} e^+e^- t\bar{c})$	$< 10^{-10}$	$O(10^{-1})$ [32]	$< 10^{-3}$	$O(1)$ [14]
$(e^+e^- \xrightarrow{Z} e^+e^- t\bar{c})$	$< 10^{-10}$	$< 10^{-3}$	$< 10^{-3}$	$< 10^{-1}$
$(e^+e^- \xrightarrow{W} e^+e^- t\bar{c})$	$< 10^{-10}$	$O(10^{-1})$ [32]	$< 10^{-3}$	$O(1)$ [14]
$Br(t \rightarrow c\gamma)$	$O(10^{-11})$ [33]	$O(10^{-5})$ [34]	$O(10^{-5})$ [9,10]	$O(10^{-4})$ [8]
$Br(t \rightarrow cZ)$	$O(10^{-13})$ [33]	$O(10^{-6})$ [34]	$O(10^{-7})$ [9,10]	$O(10^{-4})$ [8]
$Br(t \rightarrow c\gamma)$	$O(10^{-13})$ [33]	$O(10^{-7})$ [34]	$O(10^{-7})$ [9,10]	$O(10^{-6})$ [8]
$Br(t \rightarrow ch)$	$< 10^{-13}$ [33]	$O(10^{-3})$	$O(10^{-4})$ [35]	$O(10^{-1})$

For completeness we also present the branching ratios of various top rare decays in Table I. It may be surprising that the branching ratio of $t \rightarrow ch_t$ can reach 10^{-1} in TC2 model if the top-Higgs is light. In fact, this does not contradict with current experiments due to the small statistics of current top quark measurements [16,36]. Future bound on $t \rightarrow ch_t$ will not influence the optimum magnitude of $t \rightarrow c$ since the favored region for the latter process is $\sqrt{s} = 200 - 300$ GeV.

We conclude from Table I that TC2 model generally predicts much larger top quark FCNC transitions than any other models and the e^+e^- collision is the best channel in enhancing the magnitude for the top-charm associated productions at the NLC.

IV. OBSERVABILITY OF TOP-CHARM PRODUCTION AT NLC

Given the predictions listed in Table I, we now discuss their observability at the NLC. First, for the top rare decays other than $t \rightarrow ch$, the hope to observe them at the NLC is dim since only about 10^4 top quark events can be produced for an integrated luminosity of 100 fb^{-1} at the NLC [16,39]. For the top-charm associated production processes, the observability is analyzed in the following.

The cleanest signal for top-charm associated productions at the NLC is $b\bar{j} + \bar{q} + t$ with j being a light quark jet and $\bar{q} = e$ or μ . Generally speaking, the SM irreducible backgrounds for these processes are small due to the odd b-parity of the signal [37]. So far as $e^+e^- \rightarrow t\bar{c}$ is concerned, the irreducible SM background arises from $e^+e^- \rightarrow W^+W^- \rightarrow c\bar{b}$ and is negligible due to the small size of V_{cb} . The leading SM background then comes from

$$e^+e^- \rightarrow q\bar{q}^0 \quad (13)$$

where the light quark jet q or q^0 may be mis-identified as a b -jet. Such backgrounds, mainly from W pair productions as well as the W bremsstrahlung processes $e^+e^- \rightarrow W + 2 \text{ jets}$, can reach 2252 fb in total [20]. Fortunately, these

²To our knowledge, the SUSY electroweak contributions to top-charm associated production have not yet been calculated. However, from the fact that the SUSY-QCD contributions to the rare decay $t \rightarrow c$ is generally larger than SUSY electroweak contributions [9], we may infer that the SUSY-QCD contributions represent the typical size of SUSY contributions.

backgrounds can be efficiently suppressed by reconstructing the top-quark mass from the c.m. energy and the charm jet energy [20], i.e.

$$m_t^{\text{rec}} = \left(s \frac{p_{\perp}^2}{2sE_c} \right)^{1/2} \quad (14)$$

with $E_c = \frac{p_{\perp}}{2} (1 + m_t^2/s)$. According to the analysis in Ref. [20], the $t\bar{c}$ production with a cross section larger than 1 fb is observable at 95% C.L. for an integrated luminosity of 100 fb⁻¹. From Table I one sees that no new physics models can enhance the rate of $e^+e^- \rightarrow t\bar{c}$ to the level of 1 fb.

Next we turn to the process $e^+e^- \rightarrow W^+W^- \rightarrow t\bar{c}$. The signal is not as distinctive as $e^+e^- \rightarrow t\bar{c}$ due to the missing neutrinos. Its SM reducible background is generated by processes such as $e^+e^- \rightarrow W^+W^- \rightarrow e^+e^-$ and $e^+e^- \rightarrow t\bar{t} \rightarrow e^+e^-$. These backgrounds can be suppressed by applying some useful cuts [20]. So far the detailed Monte Carlo simulation for the observability of this process is still lacking. We expect conservatively that the production at the level of several fb may be accessible at the NLC. From Table I we see that TC2 model can enhance this production to this level.

Finally, we consider the $e^+e^- \rightarrow t\bar{c}$ collision. The largest SM background for $e^+e^- \rightarrow t\bar{c}$ is from $e^+e^- \rightarrow W^+W^-$, which can reach O(10) pb. Assuming a fixed c.m. energy of 500 GeV for e^+e^- collision, a detailed Monte Carlo simulation [38] showed that the background can be neglected at the expense of reducing the signal cross section to 14%. Noting the fact that the cuts used in [38] are not sensitive to the energy of e^+e^- collision, one may infer that this conclusion is approximately valid for a realistic e^+e^- collision whose c.m. energy is not fixed. In fact, this point was also emphasized at the end of Sec. III and Sec. IV in Ref. [38]. In practice, if we assume conservatively that the signal is reduced to 10% to eliminate backgrounds, we may expect that the production $e^+e^- \rightarrow t\bar{c}$ as large as 5 fb may be accessible at the NLC at 3 σ level. Compared with the predictions in Table I, one sees that TC2 model can enhance the production $e^+e^- \rightarrow t\bar{c}$ to the observable level at the NLC in a large part of the parameter space.

V. SUMMARY AND CONCLUSION

We calculated the top-charm associated productions via e^+e^- , e^+e^- and e^+e^- collisions at linear colliders in the topcolor-assisted technicolor model. Then we compared the results with the existing predictions of the SM, the general two-Higgs-doublet model and the Minimal Supersymmetric Model. We observed that the topcolor-assisted technicolor model predicts much larger production rates than other models and the largest-rate channel is $e^+e^- \rightarrow t\bar{c}$, which can exceed 10 fb for a large part of the parameter space. From the analysis of the observability of such productions at the next-generation linear colliders, we conclude that the predictions of the topcolor-assisted technicolor model can reach the observable level for a large part of the parameter space while the optimum predictions of other models may lie below the accessible level.

ACKNOWLEDGMENT

This work is supported in part by Young Outstanding Foundation of Academia Sinica, by Chinese Natural Science Foundation under No. 10175017 and by the Invitation Program of JSPS under No. L03517.

APPENDIX A: EXPRESSIONS OF THE FORM FACTORS

In this appendix, we present the expressions of the form factors c_{ij} defined in Sec. II. Here we just present the results M_i for each diagram in Fig.1. The contributions from the diagrams obtained by exchanging the two external photon lines of Fig.1 can be easily obtained by the following substitution:

$$M_i^0 = M_i(\hat{k}_1 \leftrightarrow \hat{k}_2; \hat{s} \leftrightarrow \hat{t}) \quad (A1)$$

where \hat{t} and \hat{u} are the usual Mandelstam variables defined by $\hat{t} = (p_t - k_2)^2$, $\hat{u} = (p_t - k_1)^2$. c_{ij} not listed below vanish.

Diagram (a):

$$c_{a,5} = c_{a,6} = \frac{Q_c^2}{t} (B_0^a + B_1^a); \quad c_{a,8} = 2G_{a,5}; \quad c_{a,10} = m_t c_{a,5}; \quad c_{a,19} = c_{a,20} = G_{a,5} \quad (A2)$$

where $B_1^a = B_1(p; m^+, m_b)$.

D iagram (c):

$$C_{c;5} = C_{c;6} = \frac{Q_c^2}{\hat{t} m_t^2} (B_0^c + B_1^c); \quad C_{c;8} = 2\mathcal{G}_{;5}; \quad C_{c;19} = C_{c;20} = \mathcal{G}_{;5} \quad (\text{A } 3)$$

where $B_i^c = B_i(k_2; m^+; m_b)$.

D iagram (d):

$$C_{d;1} = C_{d;4} = 4m_t \frac{Q_b Q_c}{\hat{t}} (C_{11}^d + C_{21}^d + C_{12}^d + C_{23}^d); \quad (\text{A } 4)$$

$$C_{d;5} = C_{d;6} = \frac{Q_b Q_c}{\hat{t}} [m_t^2 (C_{11}^d + C_{21}^d + C_{12}^d + C_{23}^d) + \hat{t} (C_{12}^d + C_{23}^d) + 2C_{24}^d \frac{1}{2}]; \quad (\text{A } 5)$$

$$C_{d;8} = \frac{Q_b Q_c}{\hat{t}} (4C_{24}^d + 1); \quad C_{d;18} = \frac{1}{2} C_{d;1}; \quad C_{d;19} = C_{d;20} = \mathcal{G}_{;5}; \quad (\text{A } 6)$$

$$C_{d;10} = m_t C_{d;5} + \frac{Q_b Q_c}{\hat{t}} m_t \hat{t} (C_0^d + C_{11}^d) \quad (\text{A } 7)$$

where $C_{ij}^d = C_{ij}(p; k_2; m^+; m_b; m_b)$.

D iagram (e):

$$C_{e;4} = 4m_t \frac{Q_b Q_c}{\hat{t} m_t^2} (C_{12}^e + C_{23}^e); \quad (\text{A } 8)$$

$$C_{e;5} = \frac{Q_b Q_c}{\hat{t} m_t^2} [\hat{t} (C_{12}^e + C_{23}^e) + 2C_{24}^e \frac{1}{2}]; \quad (\text{A } 9)$$

$$C_{e;6} = \frac{Q_b Q_c}{\hat{t} m_t^2} [(2m_t^2 - \hat{t}) (C_{12}^e + C_{23}^e) + 2C_{24}^e \frac{1}{2}]; \quad (\text{A } 10)$$

$$C_{e;8} = 2C_{e;5}; \quad C_{e;16} = \frac{1}{2} C_{e;4}; \quad C_{e;19} = C_{e;20} = C_{e;5} \quad (\text{A } 11)$$

where $C_{ij}^e = C_{ij}(p_c; k_1; m^+; m_b; m_b)$.

D iagram (f):

$$C_{f;1} = C_{f;4} = \frac{4m_t Q_c}{\hat{t}} (C_{11}^f + C_{21}^f + C_{12}^f + C_{23}^f); \quad (\text{A } 12)$$

$$C_{f;8} = \frac{2Q_c}{\hat{t}} [m_t^2 (C_{11}^f + C_{21}^f + C_{12}^f + C_{23}^f) + \hat{t} (C_{12}^f + C_{23}^f) + 2C_{24}^f]; \quad (\text{A } 13)$$

$$C_{f;5} = C_{f;6} = \frac{2Q_c}{\hat{t}} C_{24}^f; \quad C_{f;10} = m_t C_{f;5}; \quad C_{f;18} = \frac{1}{2} C_{f;1}; \quad C_{f;19} = C_{f;20} = \mathcal{G}_{;5} \quad (\text{A } 14)$$

where $C_{ij}^f = C_{ij}(p_c; k_2; m_b; m^+; m^+)$.

D iagram (g):

$$C_{g;4} = \frac{4m_t Q_c}{\hat{t} m_t^2} (C_{12}^g + C_{23}^g); \quad C_{g;8} = 2\mathcal{G}_{;5} = \frac{4Q_c}{\hat{t} m_t^2} C_{24}^g; \quad (\text{A } 15)$$

$$C_{g;6} = \frac{2Q_c}{\hat{t} m_t^2} [(\hat{t} - m_t^2) (C_{12}^g + C_{23}^g) + C_{24}^g]; \quad C_{g;16} = \frac{1}{2} C_{g;4}; \quad C_{g;19} = C_{g;20} = \mathcal{G}_{;5} \quad (\text{A } 16)$$

where $C_{ij}^g = C_{ij}(p_c; k_1; m_b; m^+; m^+)$.

D iagram (h):

$$C_{h;9} = m_t (C_{11}^h + C_{12}^h) \quad (\text{A } 17)$$

where $C_{ij}^h = C_{ij}(p; k_1 + k_2; m_b; m^+; m^+)$.

D iagram (i):

$$C_{i;1} = m_t Q_b^2 (4D_{21}^i \quad 4D_{24}^i \quad 4D_{25}^i + 4D_{26}^i + 4D_{31}^i + 8D_{310}^i \quad 4D_{34}^i \quad 8D_{35}^i + 4D_{38}^i \quad 4D_{39}^i); \quad (A 18)$$

$$C_{i;2} = m_t Q_b^2 (4D_{23}^i + 2D_{25}^i + 2D_{26}^i + 4D_{310}^i \quad 4D_{39}^i); \quad (A 19)$$

$$C_{i;3} = m_t Q_b^2 (2D_{25}^i + 2D_{26}^i + 4D_{310}^i \quad 4D_{35}^i + 4D_{38}^i \quad 4D_{39}^i); \quad (A 20)$$

$$C_{i;4} = 4m_t Q_b^2 (\varnothing_{11}^i \quad D_{13}^i + D_{21}^i + D_{23}^i + D_{24}^i \quad 2D_{25}^i \quad D_{26}^i \quad 2D_{310}^i + D_{34}^i + D_{39}^i); \quad (A 21)$$

$$C_{i;5} = Q_b^2 (2D_{27}^i \quad 8D_{311}^i + 2D_{312}^i + 6D_{313}^i + m_t^2 (\quad D_{11}^i + D_{12}^i \quad 3D_{21}^i \quad D_{22}^i \quad D_{23}^i + 4D_{24}^i \\ + 2D_{25}^i \quad D_{26}^i \quad 2D_{31}^i \quad 2D_{310}^i + 3D_{34}^i + 3D_{35}^i \quad D_{36}^i \quad D_{38}^i) + \mathcal{S}(\varnothing_{23}^i \quad D_{26}^i \quad 2D_{310}^i + D_{37}^i \\ + D_{39}^i) + \hat{\mathcal{C}}(D_{22}^i \quad 2D_{24}^i + D_{25}^i + D_{310}^i \quad 2D_{34}^i + D_{36}^i) + \hat{\mathcal{U}}(\varnothing_{23}^i \quad D_{26}^i + D_{310}^i \quad 2D_{35}^i + D_{38}^i)); \quad (A 22)$$

$$C_{i;6} = Q_b^2 (2D_{27}^i + 2D_{312}^i \quad 6D_{313}^i + m_t^2 (\varnothing_{11}^i + D_{12}^i \quad 2D_{13}^i + D_{21}^i \quad D_{22}^i + D_{23}^i + 2D_{24}^i \\ 3D_{25}^i + D_{34}^i \quad D_{35}^i \quad D_{36}^i + D_{38}^i) + \mathcal{S}(\quad D_{23}^i + D_{26}^i + D_{37}^i \quad D_{39}^i) + \hat{\mathcal{C}}(D_{22}^i \quad D_{26}^i \\ D_{310}^i + D_{36}^i) + \hat{\mathcal{U}}(\quad D_{23}^i + D_{25}^i + D_{310}^i \quad D_{38}^i)); \quad (A 23)$$

$$C_{i;7} = Q_b^2 (8D_{313}^i + m_t^2 (\varnothing_{25}^i \quad D_{26}^i \quad 2D_{310}^i + 2D_{35}^i \quad 2D_{38}^i) + 2D_{39}^i \mathcal{S} + D_{25}^i \hat{\mathcal{C}} + D_{26}^i \hat{\mathcal{C}} + 2D_{310}^i \hat{\mathcal{C}} \\ + 2D_{38}^i \hat{\mathcal{U}} + D_{23}^i (m_t^2 + \mathcal{S} \quad \hat{\mathcal{C}} + \hat{\mathcal{U}})); \quad (A 24)$$

$$C_{i;8} = Q_b^2 (4D_{311}^i \quad 4D_{313}^i + D_{23}^i m_t^2 \quad D_{23}^i \mathcal{S} \quad D_{23}^i \hat{\mathcal{C}} \quad D_{23}^i \hat{\mathcal{U}} \quad D_{25}^i \hat{\mathcal{U}} + D_{26}^i \hat{\mathcal{U}}); \quad (A 25)$$

$$C_{i;9} = Q_b^2 m_t (8D_{27}^i + 4D_{311}^i \quad 4D_{313}^i + D_{11}^i m_t^2 \quad D_{13}^i m_t^2 + D_{21}^i m_t^2 \quad 2D_{26}^i m_t^2 + D_{13}^i \mathcal{S} + 2D_{26}^i \mathcal{S} \\ + D_{13}^i \hat{\mathcal{C}} + 2D_{26}^i \hat{\mathcal{C}} + D_{13}^i \hat{\mathcal{U}} + D_{25}^i \hat{\mathcal{U}} + D_{26}^i \hat{\mathcal{U}} \quad (4D_{27}^i + (\varnothing_{11}^i + D_{21}^i) m_t^2)); \quad (A 26)$$

$$C_{i;10} = Q_b^2 m_t (4D_{27}^i \quad 6D_{311}^i + 6D_{313}^i + m_t^2 (\varnothing_{13}^i \quad D_{21}^i \quad D_{23}^i + D_{24}^i + 2D_{25}^i \quad D_{31}^i \quad D_{310}^i + D_{34}^i \\ + 2D_{35}^i \quad D_{38}^i) + \mathcal{S}(\quad D_{13}^i + D_{23}^i \quad D_{25}^i \quad D_{26}^i \quad D_{310}^i + D_{39}^i) + \hat{\mathcal{C}}(\quad D_{11}^i \quad D_{21}^i \\ D_{24}^i + D_{25}^i + D_{310}^i \quad D_{34}^i) + \hat{\mathcal{U}}(\quad D_{13}^i + D_{23}^i \quad 2D_{25}^i \quad D_{35}^i + D_{38}^i)); \quad (A 27)$$

$$C_{i;11} = 4Q_b^2 (\varnothing_{22}^i \quad D_{24}^i + D_{25}^i \quad D_{26}^i \quad D_{34}^i + D_{35}^i + D_{36}^i \quad D_{37}^i \quad D_{38}^i + D_{39}^i); \quad (A 28)$$

$$C_{i;12} = 4Q_b^2 (\varnothing_{23}^i \quad D_{26}^i \quad D_{37}^i + D_{39}^i); \quad (A 29)$$

$$C_{i;13} = 2Q_b^2 (\varnothing_{25}^i \quad D_{26}^i + 2(\varnothing_{310}^i \quad D_{37}^i \quad D_{38}^i + D_{39}^i)); \quad (A 30)$$

$$C_{i;14} = Q_b^2 (4D_{22}^i + 4D_{23}^i \quad 2(\varnothing_{25}^i + 3D_{26}^i + 2(\varnothing_{310}^i \quad D_{36}^i + D_{37}^i \quad D_{39}^i))); \quad (A 31)$$

$$C_{i;15} = 2Q_b^2 m_t (\quad D_{11}^i + D_{12}^i \quad D_{21}^i + D_{24}^i + D_{25}^i \quad D_{26}^i); \quad (A 32)$$

$$C_{i;16} = 2Q_b^2 m_t (\varnothing_{12}^i \quad D_{13}^i + D_{24}^i \quad D_{25}^i); \quad (A 33)$$

$$C_{i;18} = 2Q_b^2 m_t (\varnothing_{11}^i \quad D_{12}^i + D_{21}^i \quad D_{24}^i \quad D_{25}^i + D_{26}^i); \quad (A 34)$$

$$C_{i;19} = Q_b^2 (2D_{27}^i + 2D_{312}^i \quad 2D_{313}^i + m_t^2 (\quad D_{11}^i + D_{12}^i \quad D_{21}^i \quad D_{22}^i + D_{23}^i + 2D_{24}^i + D_{34}^i \quad D_{35}^i \\ D_{36}^i + D_{38}^i) + \mathcal{S}(\quad D_{23}^i + D_{37}^i \quad D_{39}^i) + \hat{\mathcal{C}}(D_{22}^i \quad D_{25}^i \quad D_{26}^i \quad D_{310}^i + D_{36}^i) \\ + \hat{\mathcal{U}}(\quad D_{23}^i \quad D_{25}^i + D_{26}^i + D_{310}^i \quad D_{38}^i)); \quad (A 35)$$

$$C_{i;20} = Q_b^2 (2D_{27}^i + 6D_{312}^i \quad 6D_{313}^i + m_t^2 (\quad D_{11}^i + D_{12}^i \quad D_{21}^i \quad D_{22}^i + D_{23}^i + 2D_{24}^i \quad D_{26}^i + D_{34}^i \quad D_{35}^i \quad D_{36}^i + D_{38}^i) \\ + \mathcal{S}(\quad D_{23}^i + D_{26}^i + D_{37}^i \quad D_{39}^i) + \hat{\mathcal{C}}(D_{22}^i \quad D_{26}^i \quad D_{310}^i + D_{36}^i) \\ + \hat{\mathcal{U}}(\quad D_{23}^i + D_{26}^i + D_{310}^i \quad D_{38}^i)); \quad (A 36)$$

where $D_{ij}^i = D_{ij}(\quad \varnothing; k_2; k_1; m_t^+; m_b; m_b; m_b)$.

D iagram (j):

$$C_{j;1} = 4Q_b m_t (\varnothing_{11}^j \quad D_{12}^j + 2D_{21}^j \quad 2D_{24}^j + D_{31}^j \quad D_{34}^j); \quad (A 37)$$

$$C_{j;2} = 4Q_b m_t (\quad D_{23}^j + D_{26}^j + D_{310}^j \quad D_{38}^j); \quad (A 38)$$

$$C_{j;3} = 4Q_b m_t (\quad D_{25}^j + D_{26}^j + D_{310}^j \quad D_{35}^j); \quad (A 39)$$

$$C_{j;4} = 4Q_b m_t (\varnothing_{12}^j \quad D_{13}^j + 2D_{24}^j \quad 2D_{25}^j + D_{34}^j \quad D_{35}^j); \quad (A 40)$$

$$C_{j;5} = 2Q_b (\varnothing_{27}^j + 4D_{311}^j \quad 4D_{312}^j + m_t^2 (\varnothing_{11}^j \quad D_{12}^j + 2D_{21}^j + D_{22}^j \quad 3D_{24}^j + D_{31}^j + D_{310}^j \quad 2D_{34}^j \\ D_{35}^j + D_{36}^j) + \mathcal{S}(\varnothing_{25}^j \quad D_{26}^j \quad D_{310}^j + D_{35}^j) + \hat{\mathcal{C}}(\quad D_{22}^j + D_{24}^j + D_{34}^j \quad D_{36}^j) + \hat{\mathcal{U}}(\varnothing_{25}^j \\ D_{26}^j + D_{310}^j \quad D_{37}^j)); \quad (A 41)$$

$$C_{j;6} = 2Q_b (\varnothing_{27}^j + 4D_{312}^j \quad 4D_{313}^j + m_t^2 (\varnothing_{12}^j \quad D_{13}^j \quad D_{22}^j + 2D_{24}^j \quad 2D_{25}^j + D_{26}^j + D_{34}^j \quad D_{35}^j \\ D_{36}^j + D_{38}^j) + \mathcal{S}(\quad D_{23}^j + D_{26}^j + D_{310}^j \quad D_{38}^j) + \hat{\mathcal{C}}(D_{22}^j \quad D_{26}^j \quad D_{310}^j + D_{36}^j) \\ + \hat{\mathcal{U}}(\quad D_{23}^j + D_{26}^j + D_{37}^j \quad D_{39}^j)); \quad (A 42)$$

$$C_{j;7} = 4Q_b D_{313}^j; C_{j;8} = 4Q_b (D_{27}^j + D_{311}^j); C_{j;9} = 4Q_b m_t (D_{27}^j + D_{311}^j); \quad (A 43)$$

$$C_{j;11} = 4Q_b (D_{22}^j D_{24}^j D_{34}^j + D_{36}^j); \quad (A 44)$$

$$C_{j;12} = 4Q_b (D_{23}^j D_{26}^j D_{37}^j + D_{39}^j); \quad (A 45)$$

$$C_{j;13} = 4Q_b (D_{25}^j D_{26}^j + D_{310}^j D_{37}^j); \quad (A 46)$$

$$C_{j;14} = 4Q_b (D_{22}^j D_{26}^j D_{310}^j + D_{36}^j); \quad (A 47)$$

$$C_{j;15} = 2Q_b m_t (D_{11}^j D_{12}^j + D_{21}^j D_{24}^j); \quad (A 48)$$

$$C_{j;16} = 2Q_b m_t (D_{12}^j + D_{13}^j D_{24}^j + D_{25}^j); \quad (A 49)$$

$$C_{j;19} = 2Q_b (D_{27}^j + 2D_{312}^j); C_{j;20} = 2Q_b D_{27}^j \quad (A 50)$$

where $D_{ij}^j = D_{ij}^j (p; k_2; p; m_t^+; m_b; m_b; m_t^+)$.

D iagram (k):

$$\alpha_{k;1} = 4m_t (D_{21}^k D_{24}^k D_{25}^k + D_{26}^k + D_{31}^k + 2D_{310}^k D_{34}^k 2D_{35}^k + D_{38}^k D_{39}^k); \quad (A 51)$$

$$\alpha_{k;2} = 4m_t (D_{23}^k D_{25}^k D_{310}^k + D_{39}^k); \quad (A 52)$$

$$\alpha_{k;3} = 4m_t (D_{310}^k + D_{35}^k D_{38}^k + D_{39}^k); \quad (A 53)$$

$$\alpha_{k;4} = 4m_t (D_{11}^k D_{13}^k + D_{21}^k + D_{23}^k + D_{24}^k 2D_{25}^k D_{26}^k 2D_{310}^k + D_{34}^k + D_{39}^k); \quad (A 54)$$

$$\alpha_{k;5} = 4D_{311}^k + 4D_{312}^k; \quad (A 55)$$

$$\alpha_{k;6} = 4(D_{27}^k + D_{312}^k); \alpha_{k;7} = 4D_{313}^k; \quad (A 56)$$

$$\alpha_{k;8} = 4(D_{27}^k + D_{311}^k D_{313}^k); \quad (A 57)$$

$$\alpha_{k;9} = 4m_t (D_{311}^k + D_{313}^k); \quad (A 58)$$

$$\alpha_{k;11} = 4(D_{22}^k D_{24}^k + D_{25}^k D_{26}^k D_{34}^k + D_{35}^k + D_{36}^k D_{37}^k D_{38}^k + D_{39}^k); \quad (A 59)$$

$$\alpha_{k;12} = 4(D_{23}^k D_{26}^k D_{37}^k + D_{39}^k); \quad (A 60)$$

$$\alpha_{k;13} = 4(D_{310}^k D_{37}^k D_{38}^k + D_{39}^k); \quad (A 61)$$

$$\alpha_{k;14} = 4(D_{12}^k D_{13}^k + D_{22}^k + D_{23}^k + D_{24}^k D_{25}^k 2D_{26}^k D_{310}^k + D_{36}^k D_{37}^k + D_{39}^k); \quad (A 62)$$

$$\alpha_{k;19} = 4(D_{312}^k D_{313}^k) \quad (A 63)$$

where $D_{ij}^k = D_{ij}^k (p; k_2; k_1; m_b; m_t^+; m_t^+; m_t^+)$.

D iagram (l): contribution from Top-pion:

$$c_{l;1} = 2Q_c^2 m_t (D_{12}^1 D_{13}^1 + D_{31}^1 + 2D_{310}^1 D_{34}^1 2D_{35}^1 + D_{38}^1 D_{39}^1); \quad (A 64)$$

$$c_{l;2} = Q_c^2 m_t (2D_{13}^1 + 2D_{23}^1 D_{25}^1 + D_{26}^1 2D_{310}^1 + 2D_{39}^1); \quad (A 65)$$

$$c_{l;3} = Q_c^2 m_t (2D_{13}^1 + D_{25}^1 D_{26}^1 + 2D_{310}^1 2D_{35}^1 + 2D_{38}^1 2D_{39}^1); \quad (A 66)$$

$$c_{l;4} = 2Q_c^2 m_t (D_{12}^1 D_{21}^1 D_{23}^1 + 2D_{25}^1 + 2D_{310}^1 D_{34}^1 D_{39}^1); \quad (A 67)$$

$$c_{l;5} = \frac{1}{2} Q_c^2 [2D_{27}^1 8D_{311}^1 + 2D_{312}^1 + 6D_{313}^1 + m_t^2 (D_{11}^1 D_{13}^1 3D_{21}^1 D_{22}^1 D_{23}^1 + 4D_{24}^1 + 2D_{25}^1 D_{26}^1 2D_{31}^1 2D_{310}^1 + 3D_{34}^1 + 3D_{35}^1 D_{36}^1 D_{38}^1) + \hat{s} (D_{23}^1 D_{26}^1 2D_{310}^1 + D_{37}^1 + D_{39}^1) + \hat{t} (D_{22}^1 2D_{24}^1 + D_{25}^1 + D_{310}^1 2D_{34}^1 + D_{36}^1) + \hat{u} (D_{23}^1 D_{26}^1 + D_{310}^1 2D_{35}^1 + D_{38}^1)]; \quad (A 68)$$

$$c_{l;6} = \frac{1}{2} Q_c^2 [2D_{27}^1 + 2D_{312}^1 6D_{313}^1 + m_t^2 (D_{11}^1 D_{13}^1 + D_{21}^1 D_{22}^1 + D_{23}^1 + 2D_{24}^1 3D_{25}^1 + D_{34}^1 D_{35}^1 D_{36}^1 + D_{38}^1) + \hat{s} (D_{23}^1 + D_{26}^1 + D_{37}^1 D_{39}^1) + \hat{t} (D_{22}^1 D_{26}^1 D_{310}^1 + D_{36}^1) + \hat{u} (D_{23}^1 + D_{25}^1 + D_{310}^1 D_{38}^1)]; \quad (A 69)$$

$$c_{l;7} = \frac{1}{2} Q_c^2 [8D_{313}^1 + m_t^2 (D_{25}^1 D_{26}^1 2D_{310}^1 + 2D_{35}^1 2D_{38}^1) + 2\hat{s} D_{39}^1 + \hat{t} (D_{25}^1 + D_{26}^1 + 2D_{310}^1) + 2D_{38}^1 \hat{u} + D_{23}^1 (m_t^2 + \hat{s} \hat{t} + \hat{u})]; \quad (A 70)$$

$$c_{l;8} = \frac{1}{2} Q_c^2 [4D_{311}^1 4D_{313}^1 + m_t^2 (2D_{11}^1 + 2D_{13}^1 + D_{23}^1) \hat{s} D_{23}^1 \hat{t} D_{23}^1 + \hat{u} (D_{23}^1 D_{25}^1 + D_{26}^1)]; \quad (A 71)$$

$$c_{i;9} = \frac{1}{2} Q_c^2 m_t (4D_{311}^1 \quad 4D_{313}^1 \quad D_{26}^1 m_t^2 + D_{26}^1 \mathfrak{s} + D_{26}^1 \hat{\mathfrak{c}} + D_{25}^1 \hat{\mathfrak{u}}); \quad (\text{A } 72)$$

$$c_{i;10} = \frac{1}{2} Q_c^2 m_t [6D_{311}^1 + 6D_{313}^1 + m_t^2 (2D_{11}^1 \quad D_{12}^1 \quad D_{13}^1 \quad D_{23}^1 + D_{25}^1 \quad D_{31}^1 \quad D_{310}^1 + D_{34}^1 \\ + 2D_{35}^1 \quad D_{38}^1) + \mathfrak{s} (D_{23}^1 \quad D_{25}^1 \quad D_{310}^1 + D_{39}^1) + \hat{\mathfrak{c}} (D_{12}^1 \quad D_{21}^1 + D_{25}^1 + D_{310}^1 \quad D_{34}^1) \\ + \hat{\mathfrak{u}} (D_{23}^1 \quad D_{25}^1 \quad D_{35}^1 + D_{38}^1)]; \quad (\text{A } 73)$$

$$c_{i;11} = 2Q_c^2 (D_{22}^1 \quad D_{24}^1 + D_{25}^1 \quad D_{26}^1 \quad D_{34}^1 + D_{35}^1 + D_{36}^1 \quad D_{37}^1 \quad D_{38}^1 + D_{39}^1); \quad (\text{A } 74)$$

$$c_{i;12} = 2Q_c^2 (D_{23}^1 \quad D_{26}^1 \quad D_{37}^1 + D_{39}^1); \quad (\text{A } 75)$$

$$c_{i;13} = Q_c^2 (D_{25}^1 \quad D_{26}^1 + 2(D_{310}^1 \quad D_{37}^1 \quad D_{38}^1 + D_{39}^1)); \quad (\text{A } 76)$$

$$c_{i;14} = Q_c^2 (2D_{22}^1 + 2D_{23}^1 \quad D_{25}^1 \quad 3D_{26}^1 \quad 2D_{310}^1 + 2D_{36}^1 \quad 2D_{37}^1 + 2D_{39}^1); \quad (\text{A } 77)$$

$$c_{i;15} = Q_c^2 m_t (D_{21}^1 + D_{24}^1 + D_{25}^1 \quad D_{26}^1); \quad (\text{A } 78)$$

$$c_{i;16} = Q_c^2 m_t (D_{13}^1 \quad D_{24}^1 + D_{25}^1); \quad (\text{A } 79)$$

$$c_{i;17} = Q_c^2 m_t D_{13}^1; \quad (\text{A } 80)$$

$$c_{i;18} = Q_c^2 m_t (D_{12}^1 + D_{13}^1 + D_{21}^1 \quad D_{24}^1 \quad D_{25}^1 + D_{26}^1); \quad (\text{A } 81)$$

$$c_{i;19} = \frac{1}{2} Q_c^2 [2D_{27}^1 + 2D_{312}^1 \quad 2D_{313}^1 + m_t^2 (D_{11}^1 + D_{13}^1 \quad D_{21}^1 \quad D_{22}^1 + D_{23}^1 + 2D_{24}^1 \\ + D_{34}^1 \quad D_{35}^1 \quad D_{36}^1 + D_{38}^1) + \mathfrak{s} (D_{23}^1 + D_{37}^1 \quad D_{39}^1) + \hat{\mathfrak{c}} (D_{22}^1 \quad D_{25}^1 \quad D_{26}^1 \\ D_{310}^1 + D_{36}^1) + \hat{\mathfrak{u}} (D_{23}^1 \quad D_{25}^1 + D_{26}^1 + D_{310}^1 \quad D_{38}^1)]; \quad (\text{A } 82)$$

$$c_{i;20} = \frac{1}{2} Q_c^2 (2D_{27}^1 + 6D_{312}^1 \quad 6D_{313}^1 + m_t^2 (D_{11}^1 + D_{13}^1 \quad D_{21}^1 \quad D_{22}^1 + D_{23}^1 + 2D_{24}^1 \quad D_{26}^1 \\ + D_{34}^1 \quad D_{35}^1 \quad D_{36}^1 + D_{38}^1) + \mathfrak{s} (D_{23}^1 + D_{26}^1 + D_{37}^1 \quad D_{39}^1) + \hat{\mathfrak{c}} (D_{22}^1 \quad D_{26}^1 \quad D_{310}^1 \\ + D_{36}^1) + \hat{\mathfrak{u}} (D_{23}^1 + D_{26}^1 + D_{310}^1 \quad D_{38}^1)]; \quad (\text{A } 83)$$

where $D_{ij}^1 = D_{ij}(p; k_2; k_1; m_t^0; m_t; m_t; m_t)$.

D iagram (l): contribution from Top-Higgs:

$$c_{i^0;1} = 2m_t Q_c^2 (D_{13}^0 \quad D_{12}^0 + 2D_{21}^0 \quad 2D_{24}^0 \quad 2D_{25}^0 + 2D_{26}^0 + D_{31}^0 + 2D_{310}^0 \quad D_{34}^0 \quad 2D_{35}^0 + D_{38}^0 \quad D_{39}^0); \quad (\text{A } 84)$$

$$c_{i^0;2} = m_t Q_c^2 (2D_{23}^0 \quad 2D_{25}^0 + D_{25}^0 + 3D_{26}^0 + 2D_{310}^0 \quad 2D_{39}^0); \quad (\text{A } 85)$$

$$c_{i^0;3} = m_t Q_c^2 (2D_{13}^0 \quad 3D_{25}^0 + 3D_{26}^0 + 2D_{310}^0 \quad 2D_{35}^0 + 2D_{38}^0 \quad 2D_{39}^0); \quad (\text{A } 86)$$

$$c_{i^0;4} = 2m_t Q_c^2 (2D_{11}^0 + D_{12}^0 \quad 2D_{13}^0 + D_{21}^0 + D_{23}^0 + 2D_{24}^0 \quad 2D_{25}^0 \quad 2D_{26}^0 \quad 2D_{310}^0 + D_{34}^0 + D_{39}^0); \quad (\text{A } 87)$$

$$c_{i^0;5} = \frac{1}{2} Q_c^2 [2D_{27}^0 \quad 8D_{311}^0 + 2D_{312}^0 + 6D_{313}^0 + m_t^2 (2D_0^0 + D_{11}^0 \quad D_{13}^0 \quad 3D_{21}^0 \quad D_{22}^0 \quad D_{23}^0 \\ + 4D_{24}^0 + 2D_{25}^0 \quad D_{26}^0 \quad 2D_{31}^0 \quad 2D_{310}^0 + 3D_{34}^0 + 3D_{35}^0 \quad D_{36}^0 \quad D_{38}^0) + \mathfrak{s} (D_{23}^0 \quad D_{26}^0 \\ 2D_{310}^0 + D_{37}^0 + D_{39}^0) + \hat{\mathfrak{c}} (D_{22}^0 \quad 2D_{24}^0 + D_{25}^0 + D_{310}^0 \quad 2D_{34}^0 + D_{36}^0) + \hat{\mathfrak{u}} (D_{23}^0 \quad D_{26}^0 \\ + D_{310}^0 \quad 2D_{35}^0 + D_{38}^0)]; \quad (\text{A } 88)$$

$$c_{i^0;6} = \frac{1}{2} Q_c^2 (2D_{27}^0 + 2D_{312}^0 \quad 6D_{313}^0 + m_t^2 (2D_0^0 + D_{11}^0 \quad D_{13}^0 + D_{21}^0 \quad D_{22}^0 + D_{23}^0 + 2D_{24}^0 \\ 3D_{25}^0 + D_{34}^0 \quad D_{35}^0 \quad D_{36}^0 + D_{38}^0) + \mathfrak{s} (D_{23}^0 + D_{26}^0 + D_{37}^0 \quad D_{39}^0) + \hat{\mathfrak{c}} (D_{22}^0 \quad D_{26}^0 \\ D_{310}^0 + D_{36}^0) + \hat{\mathfrak{u}} (D_{23}^0 + D_{25}^0 + D_{310}^0 \quad D_{38}^0)); \quad (\text{A } 89)$$

$$c_{i^0;7} = \frac{1}{2} Q_c^2 (8D_{313}^0 + m_t^2 (4D_{13}^0 \quad D_{23}^0 + D_{25}^0 \quad D_{26}^0 \quad 2D_{310}^0 + 2D_{35}^0 \quad 2D_{38}^0) + \mathfrak{s} (D_{23}^0 + 2D_{39}^0) \\ + \hat{\mathfrak{c}} (D_{23}^0 + D_{25}^0 + D_{26}^0 + 2D_{310}^0) + \hat{\mathfrak{u}} (D_{23}^0 + 2D_{38}^0)); \quad (\text{A } 90)$$

$$c_{i^0;8} = \frac{1}{2} Q_c^2 (4D_{311}^0 \quad 4D_{313}^0 + m_t^2 (4D_0^0 + 2D_{11}^0 \quad 2D_{13}^0 + D_{23}^0) \quad \mathfrak{s} D_{23}^0 \quad D_{23}^0 \hat{\mathfrak{c}} + \hat{\mathfrak{u}} (D_{23}^0 \\ D_{25}^0 + D_{26}^0)); \quad (\text{A } 91)$$

$$c_{i^0;9} = \frac{1}{2} Q_c^2 m_t (16D_{27}^0 + 4D_{311}^0 \quad 4D_{313}^0 + m_t^2 (3D_{11}^0 \quad 2D_{13}^0 + 2D_{21}^0 \quad 3D_{26}^0) + \mathfrak{s} (2D_{13}^0 + 3D_{26}^0) \\ + \hat{\mathfrak{c}} (2D_{13}^0 + 3D_{26}^0) + \hat{\mathfrak{u}} (2D_{13}^0 + D_{25}^0 + 2D_{26}^0) \quad (8D_{27}^0 + (3D_{11}^0 + 2D_{21}^0) m_t^2)); \quad (\text{A } 92)$$

$$C_{\pi^0;10} = \frac{1}{2} Q_c^2 m_t (8D_{27}^0 \quad 6D_{311}^0 + 6D_{313}^0 + m_t^2 (D_{12}^0 + D_{13}^0 \quad 2D_{21}^0 \quad D_{23}^0 + 2D_{24}^0 + 3D_{25}^0 \quad D_{31}^0 \quad (A 93)$$

$$D_{310}^0 + D_{34}^0 + 2D_{35}^0 \quad D_{38}^0) + \hat{s} (2D_{13}^0 + D_{23}^0 \quad D_{25}^0 \quad 2D_{26}^0 \quad D_{310}^0 + D_{39}^0) + \hat{t} (2D_{11}^0 \quad D_{12}^0 \quad D_{21}^0 \quad 2D_{24}^0 + D_{25}^0 + D_{310}^0 \quad D_{34}^0) + \hat{u} (2D_{13}^0 + D_{23}^0 \quad 3D_{25}^0 \quad D_{35}^0 + D_{38}^0));$$

$$C_{\pi^0;11} = 2Q_c^2 (D_{22}^0 \quad D_{24}^0 + D_{25}^0 \quad D_{26}^0 \quad D_{34}^0 + D_{35}^0 + D_{36}^0 \quad D_{37}^0 \quad D_{38}^0 + D_{39}^0); \quad (A 94)$$

$$C_{\pi^0;12} = Q_c^2 (D_{23}^0 \quad D_{26}^0 \quad D_{37}^0 + D_{39}^0); \quad (A 95)$$

$$C_{\pi^0;13} = Q_c^2 (D_{25}^0 \quad D_{26}^0 + 2(D_{310}^0 \quad D_{37}^0 \quad D_{38}^0 + D_{39}^0)); \quad (A 96)$$

$$C_{\pi^0;14} = Q_c^2 (2D_{22}^0 + 2D_{23}^0 \quad D_{25}^0 \quad 3D_{26}^0 \quad 2D_{310}^0 + 2D_{36}^0 \quad 2D_{37}^0 + 2D_{39}^0); \quad (A 97)$$

$$C_{\pi^0;15} = Q_c^2 m_t (2D_{11}^0 + 2D_{12}^0 \quad D_{21}^0 + D_{24}^0 + D_{25}^0 \quad D_{26}^0); \quad (A 98)$$

$$C_{\pi^0;16} = Q_c^2 m_t (2D_{12}^0 \quad D_{13}^0 + D_{24}^0 \quad D_{25}^0); \quad (A 99)$$

$$C_{\pi^0;17} = Q_c^2 m_t D_{13}^0; \quad C_{\pi^0;18} = Q_c^2 m_t (2D_{11}^0 \quad D_{12}^0 \quad D_{13}^0 + D_{21}^0 \quad D_{24}^0 \quad D_{25}^0 + D_{26}^0); \quad (A 100)$$

$$C_{\pi^0;19} = \frac{1}{2} Q_c^2 (2D_{27}^0 + 2D_{312}^0 \quad 2D_{313}^0 + m_t^2 (2D_{10}^0 \quad D_{11}^0 + D_{13}^0 \quad D_{21}^0 \quad D_{22}^0 + D_{23}^0 + 2D_{24}^0 + D_{34}^0 \quad (A 101)$$

$$D_{35}^0 \quad D_{36}^0 + D_{38}^0) + \hat{s} (D_{23}^0 + D_{37}^0 \quad D_{39}^0) + \hat{t} (D_{22}^0 \quad D_{25}^0 \quad D_{26}^0 \quad D_{310}^0 + D_{36}^0) + \hat{u} (D_{23}^0 \quad D_{25}^0 + D_{26}^0 + D_{310}^0 \quad D_{38}^0));$$

$$C_{\pi^0;20} = \frac{1}{2} Q_c^2 (2D_{27}^0 + 6D_{312}^0 \quad 6D_{313}^0 + m_t^2 (2D_{10}^0 \quad D_{11}^0 + D_{13}^0 \quad D_{21}^0 \quad D_{22}^0 + D_{23}^0 + 2D_{24}^0 \quad D_{26}^0 \quad (A 102)$$

$$+ D_{34}^0 \quad D_{35}^0 \quad D_{36}^0 + D_{38}^0) + \hat{s} (D_{23}^0 + D_{26}^0 + D_{37}^0 \quad D_{39}^0) + \hat{t} (D_{22}^0 \quad D_{26}^0 \quad D_{310}^0 + D_{36}^0) + \hat{u} (D_{23}^0 + D_{26}^0 + D_{310}^0 \quad D_{38}^0))$$

where $D_{ij}^0 = D_{ij}(\mathbf{p}; k_2; k_1; m_{h_t}; m_t; m_t; m_t)$.

D iagram (m): contribution from Top-pion:

$$C_{m;5} = C_{m;6} = \mathcal{G}_{m;19} = \mathcal{G}_{m;20} = \frac{1}{2} C_{m;8} = \frac{Q_c^2}{2\hat{t}} B_1^m; \quad C_{m;10} = m_t C_{m;5} \quad (A 103)$$

where $B_i^m = B_i(\mathbf{p}; m^0; m_t)$.

D iagram (m): contribution from Top-Higgs:

$$C_{m^0;5} = C_{m^0;6} = \mathcal{G}_{m^0;19} = \mathcal{G}_{m^0;20} = \frac{Q_c^2}{2\hat{t}} (2B_0^{m^0} + B_1^{m^0}); \quad (A 104)$$

$$C_{m^0;8} = 2\frac{Q_c^2}{2\hat{t}} (2B_0^{m^0} + B_1^{m^0}); \quad (A 105)$$

$$C_{m^0;10} = m_t \frac{Q_c^2}{2\hat{t}} (2B_0^{m^0} + B_1^{m^0}) \quad (A 106)$$

where $B_i^{m^0} = B_i(\mathbf{p}; m_{h_t}; m_t)$.

D iagram (n): contribution from Top-pion:

$$C_n;5 = C_n;6 = \mathcal{G}_n;19 = \mathcal{G}_n;20 = \frac{1}{2} C_n;8 = \frac{Q_c^2}{2(\hat{t} - m_t^2)} B_0^n \quad (A 107)$$

where $B_i^n = B_i(\mathbf{p}_c; m^0; m_t)$.

D iagram (n): contribution from Top-Higgs:

$$C_n^0;5 = C_n^0;6 = \mathcal{G}_n^0;19 = \mathcal{G}_n^0;20 = \frac{Q_c^2}{2(m_t^2 - \hat{t})} B_0^{n^0}; \quad C_n^0;8 = 2\frac{Q_c^2}{2(m_t^2 - \hat{t})} B_0^{n^0} \quad (A 108)$$

where $B_i^{n^0} = B_i(\mathbf{p}_c; m_{h_t}; m_t)$.

D iagram (o): contribution from Top-pion:

$$c_{o;5} = c_{o;6} = \mathcal{G}_{i;19} = \mathcal{G}_{i;20} = \frac{1}{2}c_{o;8} = \frac{Q_c^2}{2\hat{t}(\hat{t} - m_t^2)} (m_t^2 \hat{t})B_0^o \hat{t}B_1^o \quad (\text{A } 109)$$

$$c_{o;10} = \frac{Q_c^2}{2\hat{t}(\hat{t} - m_t^2)} m_t (m_t^2 \hat{t})B_0^o \quad (\text{A } 110)$$

where $B_i^o = B_i(k_2, \mathbf{p}; m^o; m_t)$.

D iagram (o): contribution from Top-Higgs:

$$c_{o;5} = \frac{Q_c^2}{2\hat{t}(\hat{t} - m_t^2)} [(m_t^2 + \hat{t})B_0^{o0} + \hat{t}B_1^{o0}]; \quad (\text{A } 111)$$

$$c_{o;6} = c_{o;5}; \quad c_{o;8} = 2\mathcal{G}_{i;5}; \quad (\text{A } 112)$$

$$c_{o;10} = m_t \frac{Q_c^2}{2\hat{t}(\hat{t} - m_t^2)} (m_t^2 \hat{t})B_0^{o0}; \quad c_{o;19} = c_{o;20} = \mathcal{G}_{i;5} \quad (\text{A } 113)$$

where $B_i^o = B_i(k_2, \mathbf{p}; m_{h_t}; m_t)$.

D iagram (p): contribution from Top-pion:

$$c_{p;1} = c_{p;4} = 4m_t \frac{Q_c^2}{2\hat{t}} (C_{12}^p + C_{21}^p - C_{23}^p); \quad (\text{A } 114)$$

$$c_{p;5} = c_{p;6} = \frac{Q_c^2}{2\hat{t}} [(m_t^2 \hat{t})(C_{12}^p + C_{23}^p) - m_t^2 (C_{11}^p + C_{21}^p) - 2C_{24}^p + \frac{1}{2}]; \quad (\text{A } 115)$$

$$c_{p;10} = \frac{Q_c^2}{2\hat{t}} m_t [\hat{t}(C_{11}^p + C_{12}^p + C_{23}^p) + m_t^2 (C_{11}^p - C_{21}^p + C_{12}^p + C_{23}^p) - 2C_{24}^p + \frac{1}{2}]; \quad (\text{A } 116)$$

$$c_{p;8} = \frac{2Q_c^2}{2\hat{t}} (m_t^2 C_{11}^p + 2C_{24}^p - \frac{1}{2}); \quad c_{p;18} = \frac{1}{2}c_{p;1}; \quad c_{p;19} = c_{p;20} = \mathcal{G}_{i;5} \quad (\text{A } 117)$$

where $C_{ij}^q = C_{ij}(k_2, \mathbf{p}; m^o; m_t; m_t)$.

D iagram (p): contribution from Top-Higgs:

$$c_{p;1} = c_{p;4} = 4m_t \frac{Q_c^2}{2\hat{t}} [2C_{11}^{p0} + C_{12}^{p0} - C_{21}^{p0} + C_{23}^{p0}]; \quad (\text{A } 118)$$

$$c_{p;5} = c_{p;6} = \frac{Q_c^2}{2\hat{t}} [\hat{t}(C_{12}^{p0} + C_{23}^{p0}) + m_t^2 (2C_0^{p0} + C_{11}^{p0} + C_{21}^{p0} - C_{12}^{p0} - C_{23}^{p0}) + 2C_{24}^{p0} - \frac{1}{2}]; \quad (\text{A } 119)$$

$$c_{p;8} = 2\frac{Q_c^2}{2\hat{t}} [m_t^2 (2C_0^{p0} + C_{11}^{p0}) - 2C_{24}^{p0} + \frac{1}{2}]; \quad (\text{A } 120)$$

$$c_{p;10} = m_t \frac{Q_c^2}{2\hat{t}} [\hat{t}(2C_0^{p0} + C_{11}^{p0} + C_{12}^{p0} + C_{23}^{p0}) + m_t^2 (2C_0^{p0} + C_{11}^{p0} + C_{21}^{p0} \quad (\text{A } 121)$$

$$C_{12}^{p0} - C_{23}^{p0}) + 2C_{24}^{p0} - \frac{1}{2}]; \quad c_{p;18} = \frac{1}{2}c_{p;1}; \quad c_{p;19} = c_{p;20} = \mathcal{G}_{i;5}$$

where $C_{ij}^{p0} = C_{ij}(k_2, \mathbf{p}; m_{h_t}; m_t; m_t)$.

D iagram (q): contribution from Top-pion:

$$c_{q;4} = 2\mathcal{G}_{i;16} = \frac{2m_t Q_c^2}{\hat{t} - m_t^2} (C_{11}^q + C_{12}^q + C_{23}^q); \quad (\text{A } 122)$$

$$c_{q;5} = \mathcal{G}_{i;19} = \mathcal{G}_{i;20} = \frac{1}{2}c_{q;8} = \frac{Q_c^2}{2(\hat{t} - m_t^2)} [\hat{t}(C_{12}^q + C_{23}^q) + 2C_{24}^q - \frac{1}{2}]; \quad (\text{A } 123)$$

$$c_{q;6} = \frac{Q_c^2}{2(\hat{t} - m_t^2)} [(\hat{t} - 2m_t^2)(C_{12}^q + C_{23}^q) - 2C_{24}^q + \frac{1}{2}]; \quad (\text{A } 124)$$

$$c_{q;10} = m_t \frac{Q_c^2}{2(\hat{t} - m_t^2)} (\hat{t} - m_t^2)C_0^q \quad (\text{A } 125)$$

where $C_{ij}^q = C_{ij}(p_c; k_i; m_c^0; m_t; m_t)$.

D iagram (q): contribution from Top-Higgs:

$$C_{q^0;4} = 4 \frac{Q_c^2}{2(\hat{t} - m_t^2)} m_t (C_{11}^{q^0} C_{12}^{q^0} C_{23}^{q^0}); \quad (\text{A } 126)$$

$$C_{q^0;5} = \frac{Q_c^2}{2(\hat{t} - m_t^2)} [\hat{t} C_{12}^{q^0} + \hat{t} C_{23}^{q^0} - 2m_t^2 C_0^{q^0} + 2C_{24}^{q^0} \frac{1}{2}]; \quad (\text{A } 127)$$

$$C_{q^0;6} = \frac{Q_c^2}{2(\hat{t} - m_t^2)} [\hat{t} (C_{12}^{q^0} + C_{23}^{q^0}) + 2m_t^2 (C_0^{q^0} + C_{12}^{q^0} + C_{23}^{q^0}) + 2C_{24}^{q^0} \frac{1}{2}]; \quad (\text{A } 128)$$

$$C_{q^0;8} = 2\mathcal{G}_{q^0;5}; \quad C_{q^0;10} = \frac{Q_c^2}{2(\hat{t} - m_t^2)} m_t (\hat{t} - m_t^2) C_0^{q^0}; \quad (\text{A } 129)$$

$$C_{q^0;16} = \frac{1}{2} C_{q^0;4}; \quad C_{q^0;19} = C_{q^0;20} = \mathcal{G}_{q^0;5} \quad (\text{A } 130)$$

where $C_{ij}^{q^0} = C_{ij}(p_c; k_i; m_{h_t}; m_t; m_t)$.

D iagram (r): contribution from Top-pion:

$$C_{r;1} = C_{r;4} = C_{r;15} = C_{r;17} = \mathcal{G}_{r;2} = \mathcal{G}_{r;3} = \mathcal{G}_{r;16} = \mathcal{G}_{r;18} = \frac{4m_t Q_c^2}{2(\hat{s} - m_t^2)} C_0^r; \quad (\text{A } 131)$$

$$C_{r;9} = \mathcal{G}_{r;10} = \frac{4m_t Q_c^2}{2(\hat{s} - m_t^2)} C_0^r \left(\frac{\hat{s}}{2} + \hat{u} \right); \quad C_{r;20} = m_t \frac{4m_t Q_c^2}{2(\hat{s} - m_t^2)} C_0^r \quad (\text{A } 132)$$

where $C_{ij}^r = C_{ij}(k_2; p_r; p_r; m_t; m_t; m_t)$.

D iagram (r): contribution from Top-Higgs:

$$C_{r^0;1} = C_{r^0;2} = C_{r^0;3} = C_{r^0;4} = \frac{4m_t Q_c^2}{2(\hat{s} - m_{h_t}^2)} (4C_{23}^{r^0} + C_0^{r^0} + 4C_{12}^{r^0}) \quad (\text{A } 133)$$

$$C_{r^0;9} = \frac{4m_t Q_c^2}{2(\hat{s} - m_{h_t}^2)} [\hat{s} \left(\frac{1}{2} C_0^{r^0} C_{12}^{r^0} C_{23}^{r^0} \right) + m_t^2 C_0^{r^0} + \frac{1}{2}] \quad (\text{A } 134)$$

where $C_{ij}^{r^0} = C_{ij}(k_2; k_i; m_t; m_t; m_t)$.

In above expression, Q_c and Q_b are the charges of charm and bottom quark, respectively, and we adopted the conventions of Ref. [40] for 3-point Feynman integrals C_{ij} and 4-point Feynman integrals D_{ij} .

- [1] For model-independent analyses, see, e.g., C. T. Hill and S. J. Parke, Phys. Rev. D 49, 4454 (1994); K. Whisnant, et al., Phys. Rev. D 56, 467 (1997); K. Hikasa, et al., Phys. Rev. D 58, 114003 (1998).
- [2] See, e.g., C. T. Hill, Phys. Lett. B 345, 483 (1995); K. Lane, E. Eichten, Phys. Lett. B 352, 382 (1995); K. Lane, Phys. Lett. B 433, 96 (1998); G. Cvetič, Rev. Mod. Phys. 71, 513 (1999).
- [3] A. Datta, et al., Phys. Rev. D 56, 3107 (1997); R. J. Oakes, et al., Phys. Rev. D 57, 534 (1998); K. Hikasa, J. M. Yang, B.-L. Young, Phys. Rev. D 60, 114041 (1999); P. Chiappetta, et al., Phys. Rev. D 61, 115008 (2000);
- [4] M. Hirsch, et al., Phys. Rev. D 58, 034002 (1998); S. Mrenna and C. P. Yuan, Phys. Lett. B 367, 188 (1996). K. J. Abraham, et al., Phys. Lett. B 514, 72 (2001); Phys. Rev. D 63, 034011 (2001); F. del Aguila, J. A. Aguilar-Saavedra, R. Miquel, Phys. Rev. Lett. 82, 1628 (1999);
- [5] H. J. He and C. P. Yuan, Phys. Rev. Lett. 83, 28 (1999); G. Burdman, Phys. Rev. Lett. 83, 2888 (1999).
- [6] J. Cao, Z. Xiong and J. M. Yang, Phys. Rev. D 67, 071701 (2003); F. Larios and F. Penunuri, hep-ph/0311056.
- [7] C. Yue, et al., Mod. Phys. Lett. A 17, 2349 (2002); X. Wang, et al., Phys. Rev. D 66, 075009 (2002).
- [8] For FCNC top quark decays in TC2 theory, see, X. L. Wang et al., Phys. Rev. D 50, 5781 (1994); C. Yue, et al., Phys. Lett. B 508, 290 (2001); G. Lu, F. Yin, X. Wang and L. Wan, Phys. Rev. D 68, 015002 (2003).
- [9] For FCNC top quark decays in the MSSM and TC, see, C. S. Li, R. J. Oakes and J. M. Yang, Phys. Rev. D 49, 293 (1994); G. Couture, C. Hamzaoui and H. Konig, Phys. Rev. D 52, 1713 (1995); J. L. Lopez, D. V. Nanopoulos and R. Rangarajan, Phys. Rev. D 56, 3100 (1997); G. M. de Divitiis, R. Petronzio and L. Silvestrini, Nucl. Phys. B 504, 45 (1997). J. M. Yang,

- B.-L. Young and X. Zhang, *Phys. Rev. D* 58, 055001 (1998); J. M. Yang and C. S. Li, *Phys. Rev. D* 49, 3412 (1994); J. Guasch, and J. Sola, *Nucl. Phys. B* 562, 3 (1999); G. Eilam, et al, *Phys. Lett. B* 510, 227 (2001).
- [10] For top-charm associated productions in the M SSM, see: J. Cao, Z. Xiong and J. M. Yang, *Nucl. Phys. B* 651, 87 (2003); C. S. Li, X. Zhang and S. H. Zhu, *Phys. Rev. D* 60, 077702 (1999).
- [11] Y. Zeng-Hui, et. al, *Euro. Phys. J. C* 16, 541 (2000).
- [12] J. Yi, et. al, *Phys. Rev. D* 57, 4343 (1998).
- [13] C. Yue, et al, *Phys. Lett. B* 525, 301 (2002).
- [14] C. Yue, G. Liu and Q. Xu, *Phys. Lett. B* 509, 294 (2001).
- [15] C. Yue, et al *Phys. Lett. B* 496, 93 (2000).
- [16] For recent reviews on top quark, see, e.g., C. T. Hill and E. Simons, *hep-ph/0203079*; C.-P. Yuan, *hep-ph/0203088*; E. Simons, *hep-ph/0211335*; S. Willenbrock, *hep-ph/0211067*; D. Chakraborty, J. Konigsberg, D. Rainwater, *hep-ph/0303092*.
- [17] K. Abe et al, ACFA Linear Collider Working Group, *hep-ph/0109166*.
- [18] S. J. Brodsky, T. Kinoshita and H. Terazawa, *Phys. Rev. D* 4, 1532 (1971); H. Terazawa, *Rev. Mod. Phys.* 45, 615 (1973); B. A. Kniehl, *Phys. Lett. B* 254, 267 (1991).
- [19] R. Cahn and S. Dawson, *Phys. Lett. B* 136, 196 (1984); M. Chanowitz and M. K. Gaillard, *Phys. Lett. B* 142, 85 (1984); G. L. Kane, et. al, *Phys. Lett. B* 148, 367 (1984).
- [20] T. Han and J. L. Hewett, *Phys. Rev. D* 60, 074015 (1999); S. Bar-Shalom and J. Wudka, *Phys. Rev. D* 60, 094016 (1999); J. A. Aguilar-Saavedra, *Phys. Lett. B* 502, 115 (2001); J. A. Aguilar-Saavedra, T. Riemann, *hep-ph/0102197*.
- [21] I. F. Ginzburg, et al, *Nucl. Instrum* 219, 5 (1984); V. I. Tehov, *Nucl. Instrum. Meth* 294, 72 (1990).
- [22] R. S. Chivukula, B. Dobrescu, H. Georgi and C. T. Hill, *Phys. Rev. D* 59, 075003 (1999).
- [23] Particle Physics Group. *Euro. Phys. J. C* 15, 274 (2000).
- [24] G. Burdman and D. Komaris, *Phys. Lett. B* 403, 101 (1997); C. Yue, Y. P. Kuang, X. Wang and W. Li, *Phys. Rev. D* 62, 055005 (2000).
- [25] T. P. Cheng and M. Sher, *Phys. Rev. D* 35, 3484 (1987); L. J. Hall and S. Weinberg, *Phys. Rev. D* 48, 979 (1993).
- [26] D. Atwood, L. Reina and A. Soni, *Phys. Rev. D* 54, 3296 (1996); D. Atwood, L. Reina and A. Soni, *Phys. Rev. D* 55, 3156 (1997); L. Reina, *hep-ph/9712426*; M. Sher, *hep-ph/9809590*; D. Bowser-Chao, K. Cheung and W. Y. Keung, *Phys. Rev. D* 59, 115006 (1999).
- [27] H. E. Haber and G. L. Kane, *Phys. Rept.* 117, 75 (1985); J. F. Gunion and H. E. Haber, *Nucl. Phys. B* 272, 1 (1986).
- [28] L. J. Hall, R. Rattazzi and U. Sarid, *Phys. Rev. D* 50, 7048 (1994); T. Blazek, S. Raby and S. Pokorski, *Phys. Rev. D* 52, 4151 (1995); M. Carena, S. Mrenna and C. E. M. Wagner, *Phys. Rev. D* 60, 075010 (1999); K. S. Babu and C. F. Kolda, *Phys. Lett. B* 451, 77 (1999); *Phys. Rev. Lett.* 84, 228 (2000).
- [29] See, e.g., M. Misiak, S. Pokorski and J. Rosiek, *Adv. Ser. Direct. High Energy Phys.* 15, 795 (1998); K. Hikasa and M. Kobayashi, *Phys. Rev. D* 36, 724 (1987).
- [30] C. S. Huang, X. H. Wu and S. H. Zhu, *Phys. Lett. B* 452, 143 (1999).
- [31] D. Atwood, L. Reina and A. Soni, *Phys. Rev. D* 53, 1199 (1996).
- [32] S. Bar-Shalom, G. Eilam, A. Soni and J. Wudka, *Phys. Rev. Lett.* 79, 1217 (1997); S. Bar-Shalom, G. Eilam, A. Soni and J. Wudka, *Phys. Rev. D* 57, 2957 (1998).
- [33] G. Eilam, J. L. Hewett and A. Soni, *Phys. Rev. D* 44, 1473 (1991); B. Mele, S. Petrarca and A. Soddu, *Phys. Lett. B* 435, 401 (1998).
- [34] D. Atwood, L. Reina and A. Soni, *Phys. Rev. D* 55, 3156 (1997); R. A. Diaz, R. Martinez and J. A. Rodriguez, *hep-ph/0103307*.
- [35] J. Guasch and J. Sola, *hep-ph/9909503*; S. Bejar, J. Guasch and J. Sola, *Nucl. Phys. B* 600, 21 (2001).
- [36] F. Abe et al, CDF Collaboration, *Phys. Rev. Lett.* 80, 2525 (1998); J. A. Aguilar-Saavedra, G. C. Branco, *Phys. Lett. B* 495, 347 (2000);
- [37] S. Bar-Shalom and J. Wudka, *Phys. Rev. Lett.* 86, 3722 (2001).
- [38] K. J. Abraham, K. Whisnant and B.-L. Young, *Phys. Lett. B* 419, 381 (1998).
- [39] R. Frey et al, FERMILAB-CONF-97-085 (1997); *hep-ph/9704243*.
- [40] A. Axelrod, *Nucl. Phys. B* 209, 349 (1982).